Technische Universität München

Master's Thesis

Design and Analysis of a Hybrid Renewable Microgrid System for Humanitarian Help

written by

Denim Dheeraj D'costa
Matr.Nr. 03658392

submitted to the

Lehrstuhl für Energiewirtschaft und Anwendungstechnik
Technische Universität München,

Prof. Dr.-Ing. Ulrich Wagner

In cooperation with

United Nation's World Food Programme

Advisors: **Prof. Dr.-Ing. Ulrich Wagner (TUM)**
Mr. Matthew Allen (WFP HQ, Rome)

Abstract

World Food Programme (WFP) is the world's largest humanitarian aid organization and United Nations (UN) frontline relief agency. Throughout WFP humanitarian operations at remote locations, there is a wide range of energy need which relies heavily on diesel generators where the national grid is either absent or unstable.

Due to the increase in prices of petroleum products, CO_2 emission awareness and developments in renewable energy technologies, Hybrid Energy systems (combination of two or more energy systems) are gaining popularity to meet the energy/electricity demand of decentralized networks. In the remote rural areas of a developing country, grid-based electricity supply is still a significant challenge, and decentralized hybrid renewable microgrid system is a better alternative to meet the energy demand in an environmentally friendly way by reducing dependency on diesel fuel. The reliability of such a hybrid system can further be improved by integrating renewable sources with diesel generators and storage.

With an increasing focus on green energy solution within UN and the humanitarian community at large, this thesis aims to achieve a cost-effective solution to meet the electricity demand with renewable energy technology combination including battery storage at WFP locations. To meet the electricity demand, along with the design of small portable Type I systems, energy system modeling is carried out for Type II hybrid microgrid system by the integration of various renewable energies like solar, wind and micro-hydro into modeling tool along with microgrid controller, batteries, diesel generators and unreliable grid parameters. The business case is developed to analyze the cost savings, payback period and reduction in CO_2 emissions which can help improve WFP's net effectiveness in supporting beneficiaries.

Lehrstuhl für Energiewirtschaft und Anwendungstechnik
Fakultät für Elektrotechnik und Informationstechnik
Technische Universität München

Aufgabenstellung
Master´s Thesis
von
Herrn D`COSTA, Denim Dheeraj
Matr.-Nr. 03658392

Design and Analysis of a Hybrid Renewable Microgrid System for Humanitarian Help

Design und Analyse eines hybriden Stromerzeugungssystems mittels erneuerbarer Energie für humanitäre Hilfe

For a reliable and clean energy supply for humanitarian aid companies the development of renewable, off-grid energy systems is necessary. This includes solar, wind and biomass based systems for use in remote regions or affected communities where the national grid is absent or unstable.

The scope of this Master's Thesis includes the following tasks:

- Comprehensive literature review on current research activities, technological solutions and initiatives Comparative analysis of technologies in use (efficient and safe construction and operation)
- Assessment (potential field survey) of field locations and their potential for renewable energies
- Conceptual design of an energy system suitable for hybrid power supplies
  - Type I, fast response energy supply (power range 1-2 kW per unit), max. 32 kg per item
  - Type II, long-term installation (power range 10-100 kW), transportable by cargo aircraft
  - Universal applicability (unstable grid, energy storage, modularity, maintenance, costs etc.)

The thesis is carried out in close cooperation with experts of the World Food Programme (WFP), who contribute information on typical applications. Final goal is a simulation program for the electricity demand and generation, finding a cost-optimized renewable power generation technology.

Betreuer:	Prof. Dr.-Ing. Ulrich Wagner.	Tel.: 089-289 28301
Ausgabedatum:	02.10.2017	
Aufgabensteller:		U. Wagner Prof. Dr.-Ing. Ulrich Wagner

Statement of Academic Integrity

I,
Last name: D’costa
First name: Denim Dheeraj
ID No.: 03658392

hereby confirm that the attached thesis,

Design and Analysis of a Hybrid Renewable Microgrid System for Humanitarian Help

was written independently by me without the use of any sources or aids beyond those cited, and all passages and ideas taken from other sources are indicated in the text and given the corresponding citation.
Tools provided by the institute and its staff, such as models or programs, are also listed. These tools are the property of the institute or of the individual staff member. I will not use them for any work beyond the attached thesis or make them available to third parties.

I agree with the further use of my work and its results (including programs produced and methods used) for research and instructional purposes.

I have not previously submitted this thesis for academic credit.

Munich, 22.05.2018

Denim

Dcosta, Denim Dheeraj

Table of Contents

1. Introduction and Motivation

More than 1billion people in this world do not have access to electricity. Most of them are located in remote rural locations of developing countries predominantly in sub-Saharan Africa and parts of Asia (India) [1]. One of the reasons being, most of the time the national grid is absent or unstable at these locations which forces them to rely heavily on diesel generators to meet energy needs which are not only expensive and vulnerable to the fluctuating fuel prices but also pollutes our environment. United Nations Sustainable Development Goals (SDG 7) aims at ensuring access to affordable, reliable, sustainable and modern energy for all.

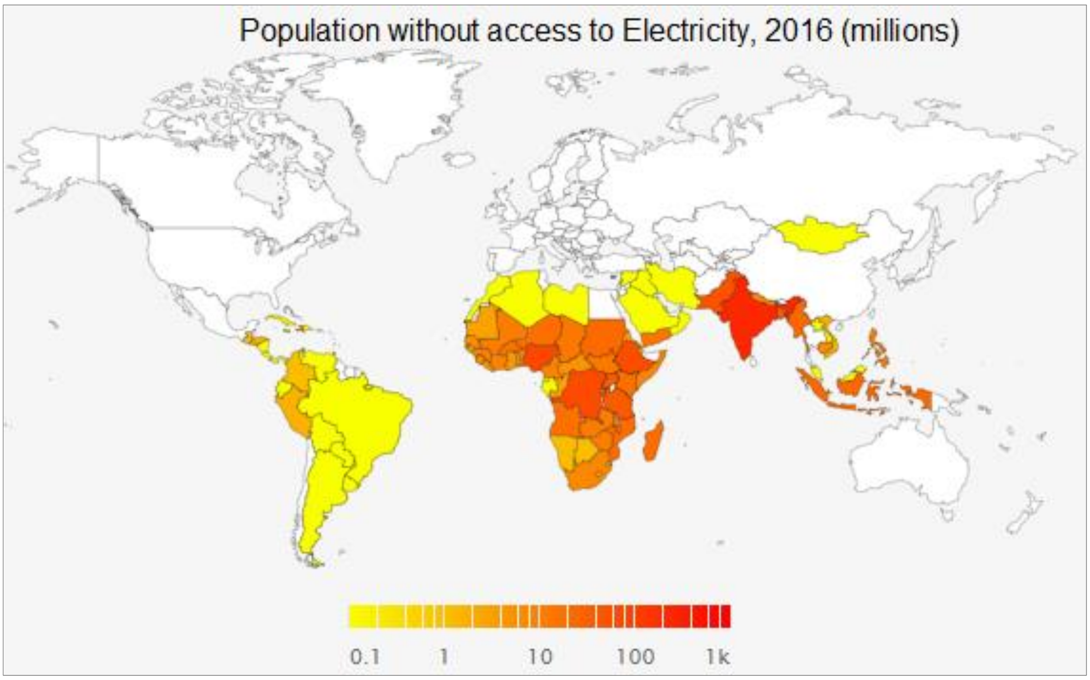

Figure 1: World Without Electricity **[2]**

World Food Programme (WFP) is one of the world's largest United Nations humanitarian aid organization fighting hunger worldwide. They are present in more than 80 countries providing food assistance to more than 80 million people worldwide. They are operating in war zones, disasters and protracted crisis regions. WFP has more than 15000 staff, and 90% of them are deputed across field locations.

Most of the WFP humanitarian facilities are located in remote locations of developing countries where the national grid is absent or unstable. More than 300 WFP office locations are completely off-grid and are running on diesel generators only, which results in burning more than 6.1 million liters of generator fuel to power WFP offices worldwide. This is an expensive and environmentally unsustainable way of producing power, causing harm to the environment, increasing the cost of humanitarian operations, and reducing WFP's net effectiveness in supporting beneficiaries.

For Long-term reliable and clean energy supply, WFP seeks to identify sustainable alternatives and to accelerate the design and development of renewable energy solutions for use in remote WFP locations with unstable/unreliable/no grid and continue efforts by the UN in reducing fossil fuel energy consumption and environmental impact [3], [4].

With the declining cost of renewables, innovation, and improvement in technologies and energy efficiency, decentralized hybrid renewable systems have become an attractive, cost-effective solution at locations which are off-grid or connected with unreliable grid [1], [5], [6], [7]. This thesis aims at developing a concept design and analysis of hybrid renewable systems to meet the energy demand at WFP humanitarian office locations in energy efficient, environmentally friendly way and thereby achieve a reduction in operating cost by reducing dependency on diesel fuel. With the cost savings achieved, WFP can help feed more children suffering from hunger worldwide.

This Concept design of the systems is subdivided into Type I and Type II systems. Type I systems are small portable systems to power biometric verification devices for the limited duration of time. For Type I system, design and analysis were carried out with different configurations based on battery capacity and weight constraints.

Type II systems are hybrid renewable microgrid systems to power WFP offices at remote locations. For Type II system,

1) The first step was to understand the hourly load profile for a year at one of the WFP humanitarian locations. Various contributors to this load profile would be lighting, heating, refrigeration, office equipment, etc.
2) In the second step, considering both as off-grid and on-grid system, energy system modeling was carried out to meet the electricity demand by the integration of renewable energies which includes the integration of hourly analysis of solar, wind and micro-hydro into modeling tool along with the controller, diesel generators, and batteries. The system was analyzed by Homer Pro microgrid simulation software developed by NREL (National Renewable Energy Laboratory) taking into account the efficiency and cost parameters of the selected technologies.
3) The third step was to investigate the best hybrid system configuration along with sensitivity analysis, taking into account unreliable grid parameters and existing generators to determine the optimum capacity of renewables and battery storage to store the excess energy input from the above-mentioned system and the extent to which this can replace expensive diesel fuel. In the final stage, a business case was developed to analyze the cost savings, payback period and reduction in CO_2 emissions.

Further, market research was also carried out to identify key equipment suppliers for both Type I and Type II systems.

2. WFP Energy System Requirements and Energy Efficiency Programme

2.1 WFP System Energy Requirements

WFP energy system requirements are divided into two categories, known as Type I and Type II systems based on the application and kW rating.

2.1.1 Type I Systems:

Figure 2: Biometric Data Collection, WFP SCOPE

SCOPE is WFP's central repository for beneficiary data collection and verification. SCOPE allows for a considerable increase in efficiency over traditional paper-based methodology. SCOPE is compatible with all WFP transfer modalities such as a voucher, cash, and barcoded card. The registration process involves collecting biometric data using laptops and other biometric verification devices etc. The entire registration process at each location (i.e., up to 1,500 households) currently takes about one month. Access to **800 watts of energy for 8hrs/day (b/w 9 to 17 hrs.)** to power these devices could reduce that period, using the same team of five staff, to just a few days [4].

WFP requirement is Type I fast response portable system carried as checked baggage with a max weight of approx. b/w 32 to 40 kg to meet energy needs as mentioned above. Concept design of Type I system with three different configurations will be analyzed in chapter 4.

2.1.2 Type II Systems:

Figure 3: WFP OFF-GRID Locations **[3]**

Figure 3 shows WFP's facilities at off-grid humanitarian locations. More than 300 WFP offices are completely off-grid and running on diesel generators only. Some of the offices are connected to the unstable/unreliable grid and hence heavily dependent on diesel fuel to meet load during outage/blackout. This is an expensive and environmentally unsustainable way of producing power, causing harm to the environment, increasing the cost of humanitarian operations, and reducing WFP's net effectiveness in supporting beneficiaries [3].

For long-term, reliable and clean energy supply, WFP seeks to accelerate the design and development of hybrid renewable energy microgrid systems to implement in remote regions or affected communities where national grid is unstable or absent. WFP is looking for solutions that could potentially include the design of new systems as well as the improvement or integration of existing technologies [8]. Concept design of Type II system considering both as off-grid and grid connected with unreliable grid parameters along with the business case for one of the WFP location will be analyzed in detail in chapter 5, 6 and 7 respectively.

2.2 Energy Efficiency Program (EEP)

The Energy Efficiency Programme (EEP) which is being implemented by the WFP engineering team provides support to WFP offices worldwide in producing energy more efficiently thereby reducing cost and environmental impact because of CO_2 emissions.

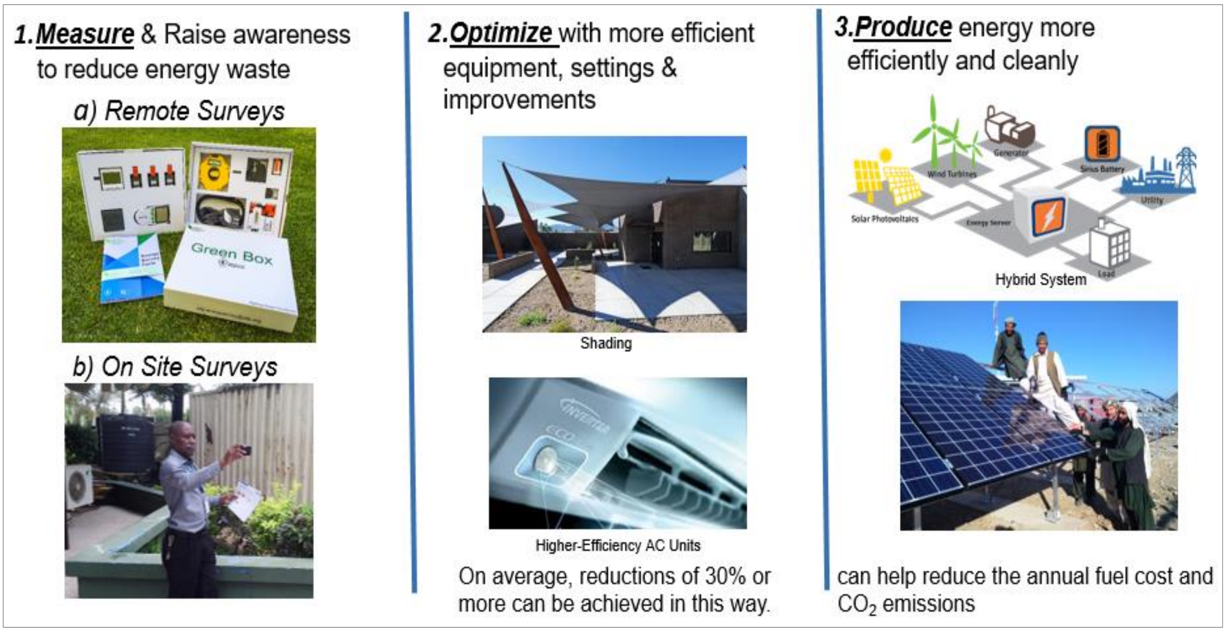

Figure 4: WFP EEP MOP UP Waste Concept **[3]**

The EEP supports Country Offices by surveying electricity production, distribution, and usage in WFP facilities. The entire process is termed as MOP UP waste, which stands for measure, optimize and producing energy more efficiently.

The energy efficiency survey process is carried out to gather data and to understand the electrical load/usage pattern which would help in developing a cost-effective solution to optimize and produce energy more efficiently. Information is collected from three data sources as follows

- Through an onsite survey or by office staff providing information on the power supply, electrical distribution, equipment rating and consumption information.

- Through remote surveys using an energy monitor, known as Green Box which was jointly developed by WFP engineering and environmental sustainability unit in collaboration with WFP innovative accelerator in Munich. The green kit can be easily set up without the requirement for engineers from WFP HQ, and the electrical consumption is remotely monitored and recorded either while on-site or streamed through a web connection, providing continuous live readings [9].

- Through administrative records, providing information on generator fuel and grid electricity consumption.

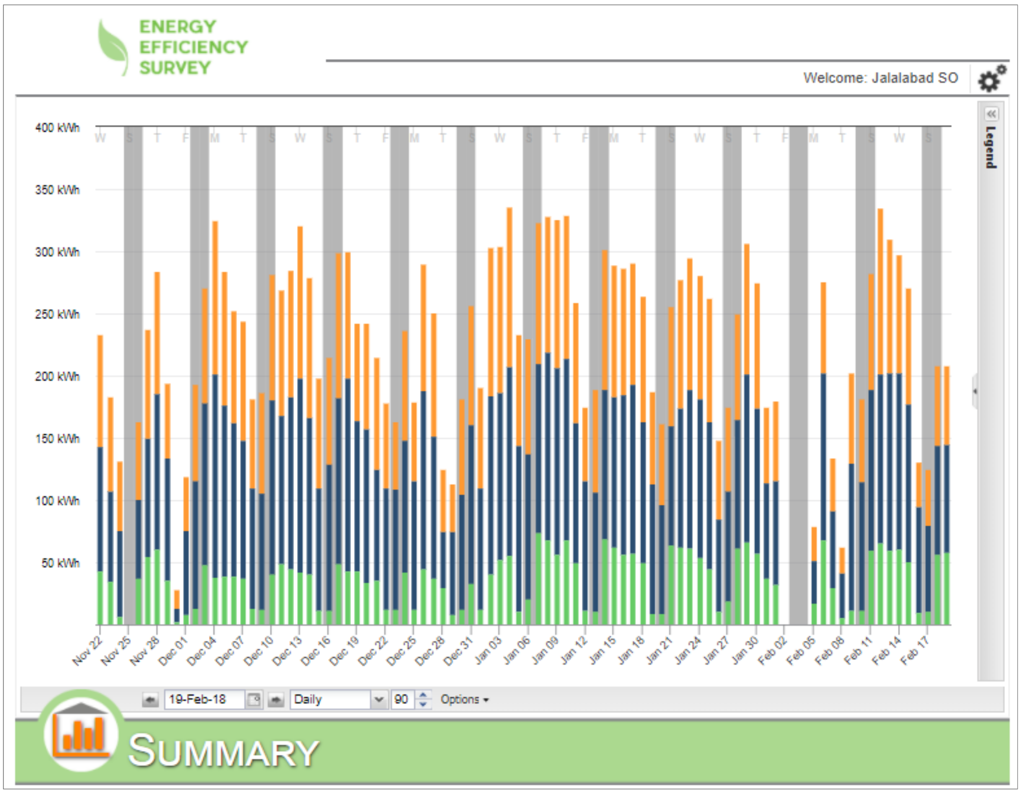

Figure 5: Remote Survey using Energy Monitor - Green Box **[10]**

Combining and comparing these different sources of data provides a good overview of the current energy consumption profile and makes it possible to identify possibilities of upgrading to energy efficient equipment's and also installing renewable systems to reduce carbon footprints [3], [11]. In this thesis report, all the data available from WFP will be analyzed for one of the WFP site locations and the load profile for the whole year will be estimated as discussed in section 5.3 to investigate further feasibility of installing hybrid renewable microgrid systems.

3. Feasibility Analysis of Renewable Energy Systems and Energy Storage

In this chapter, the feasibility of renewable energy systems to power WFP offices at humanitarian locations will be briefly analyzed. Market research on a comparison of currently available technologies will not be included in this report as it has already been covered by Mr. Quirin Strobel in his bachelor thesis report titled “Auxiliary Power Units for Developing Countries - Evaluation of Selected Renewable Energy Systems.”

3.1 Solar

Energy from the sun can be harnessed to generate electricity, heating, etc. With the cost of solar panels/ modules declining over 80% in the past seven years (2009-2016) [12], solar energy is considered to be a low cost renewable energy technology and soon predicted be cheapest form of electricity in many regions of the world playing a major role in electricity production in future [6].

One of the ways to convert sunlight into electricity is by photovoltaic conversion. A photovoltaic (PV) module is formed when individual solar cells are electrically connected together to increase their power output. There are various types of solar cells ranging from crystalline silicon, thin film, III and IV generation solar cells which include organic and dye-sensitized solar cells [13]. Most widely used solar cells are mono and polycrystalline silicon because of cost-effectiveness and efficiency when compared to other types [14], [15].

As shown in Figure 3, most of the WFP off-grid humanitarian locations running only on diesel generators are in developing countries including sub-Saharan Africa and parts of Asia having high solar irradiance which makes it possible to design and implement solar PV technologies to achieve cost savings and reduction in fuel consumption. Hence, detailed feasibility analysis and concept design of solar PV system for one of the WFP locations has been discussed further in section 5.4.

3.2 Wind

The kinetic energy of the wind is utilized to generate electricity using wind turbine. The amount of energy generated from the wind depends on the diameter of the rotor and cube of wind speed [16].

International Electrotechnical Commission (IEC) defines a small wind turbine as having a rotor swept area of less than 200 square meters, equating to a rated power of some 50 kW. The capital cost per kW of a small wind turbine is higher and has a lower efficiency when compared to big wind farms. However, in the regions where expensive diesel generators are used, small wind turbines are beneficial for electricity storage or off-grid electricity supply and water pumping in rural/grid-isolated areas [17].

Assessing the wind resource is one of the major challenges in installing the wind turbine. Smaller wind turbines have similar resource assessment process to that for larger turbines; however, it is expensive due to the high cost of management tools and long-term measurement efforts. The planning cost per unit installed for smaller wind turbine increases dramatically because of their installation as stand-alone units and not as wind farms. The height of the tower(<30m) is also a key factor for small wind turbines to reduce the turbulence caused by surrounding obstacles which in turn further leads to higher cost [17].

As discussed with WFP engineering team Rome, the possibility of installing small wind turbines were considered not to be favorable during the emergency response process analyzing difficulties w.r.t wind resource assessment of the site and installation drawbacks. However, cost-benefit analysis has been performed for one of the WFP site locations to evaluate the feasibility of installing small capacity wind turbines in section 5.5 and 6.4.5.

3.3 Micro-hydro

Mobile micro-hydro/ water stream turbine is a potential technology for producing electricity in an environmentally friendly way without any complex structures likes dams or weirs. It utilizes kinetic energy of the flowing waters [18]. The amount of kinetic velocity varies from river/canal, a greater amount of energy is generated with a varying velocity of water flow [19].

Most of the WFP operational sites do not have access to the river and are not located close to the flowing water stream, however, at the very limited location, there are still possibilities to install such systems. Micro-hydro system feasibility analysis including the effect of water flow velocity on hydrokinetic turbine output has been discussed in section 5.6 and 6.4.6.

3.4 Biomass

In comparison to the PV and wind power, biomass power technology can generate continuous power output using many agricultural wastes, forest residues and farmers can generate income by selling biomass fuels for the local power plant. Despite all the apparent benefits, such technologies have been very rarely implemented for small-scale electricity generation in off-grid areas of developing countries. The potential savings from high-cost commercial fuel to locally available low-cost biomass has to be compensated with the higher costs for the initial investment, labor, operation, and maintenance [20].

As per the extensive studies conducted by Deutsche Gesellschaft für Internationale Zusammenarbeit(GIZ) GmbH, it was found that "there is not yet any reliable, affordable standard gasifier technology appropriate for rural small-scale applications." Even though the technology sounds reasonable in some industrial application with continuous technical support, it is not feasible for mere communal purposes and providing electricity to households and small businesses in remote areas [20].

In many humanitarian setting, especially in areas with scarce natural resources, host communities and displaced populations often compete for access to fuel and energy resources. The fuel needs of crisis-affected populations leading to deforestation and forest degradation can increase the risk of disasters caused by natural hazards [21]. As discussed with WFP team Rome, due to high maintenance and complex management of such system (including carcinogenic waste), biomass-based small-scale electrification will not be considered for this project.

3.5 Energy Storage

Most of the renewable energy resources are intermittent in nature which poses a greater challenge in term of reliability to ensure continuous power supply. Electrical energy storage (EES) is considered to be one of the promising solutions to address this problem. Electrical energy storage is the process of converting electrical energy to a storable form and reserving it in various forms and then converting back to electrical energy when needed. The distinct value proposition of EES includes load balancing, peak shaving, improving power quality and reliability, increase renewable share, energy time shift (arbitrage), etc. [22].

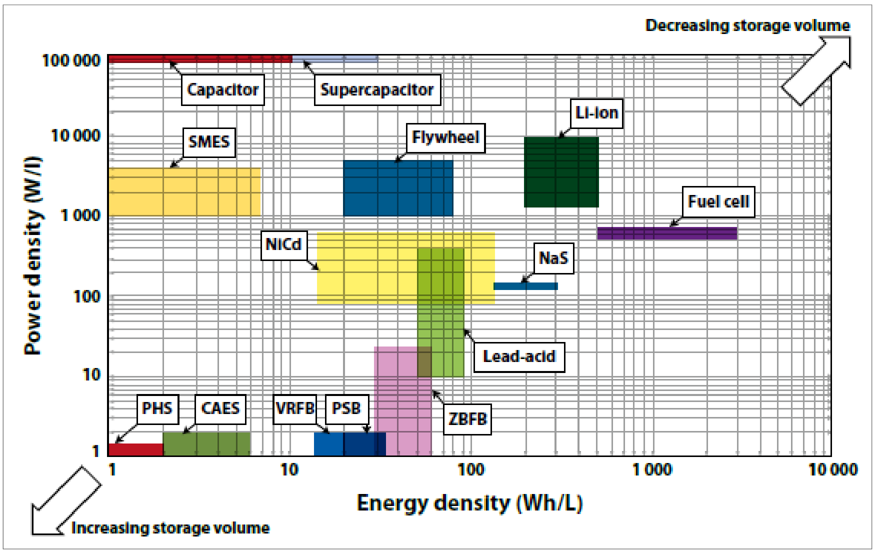

Figure 6: Ragone Plot for Energy Storage Technologies **[22]**

Note: SMES = superconducting magnetic energy storage; NiCd = nickel cadmium; NaS = sodium sulphur; PHS = pumped hydro storage; CAES = compressed air energy storage; VRFB = vanadium redox flow battery; PSB= polysulfide bromine flow battery; ZBFB = zinc bromine flow battery; Li-Ion = lithium ion.

Ragone plot is used for performance comparison of various storage energy technologies. Depending on the discharge times (i.e., seconds to hours) and the power rating (i.e., ranging from kW to GW order), appropriate, suitable technologies are selected. The technologies with higher power and energy density signify that small volume is feasible, conversely, with lower power and energy density, large volumes are required and are not suitable for volume constrained application [22]. Since most of the WFP humanitarian locations are remotely connected, the storage technologies with high power and energy density are of utmost importance which can help in ease of transportation along with reducing the storage volume requirements.

Remote/off-grid areas are considered to be one of the most attractive options for implementation of battery storage to integrate variable renewable energy. Most of the WFP off-grid locations are running on diesel generators which are oversized to meet the peak demand and are restricted to operate below 25% of capacity. Implementation of battery storage can help the integration of renewable energy and reduce dependence on diesel fuel which is vulnerable to fluctuating diesel prices [7].

There are different types of rechargeable batteries, i.e., flow batteries, lead acid, lithium ion, etc. Flow batteries require higher maintenance because of the circulation of the electrolyte solution requiring pumping, sensors and flow mechanism controls, etc. Even though lithium-ion batteries have higher upfront cost compared to lead acid batteries, they have advantages w.r.t high specific energy, high energy density, life cycle, depth of discharge (DOD), efficiency, low self-discharge, etc. [23], [24].

Any evaluation of energy storages is therefore not universally valid and depends on the conditions of the regarded application such as application, cycle life, costs, safety, performance guarantee, maintenance requirement, ambient operating conditions, depth of discharge, technology track record, etc. [24]. After analyzing all the parameters, it was observed that lithium-ion batteries are suitable to meet WFP requirements. The cost of lithium-ion batteries has fallen as much as 73% between 2010 to 2016, and it is estimated that the cost could further decrease by more than 50% by 2030 in stationary application [25].

There are various types of lithium-ion chemistries such as nickel cobalt aluminum (NCA), nickel manganese cobalt (NMC), lithium manganese oxide (LMO), lithium iron phosphate(LFP), lithium titanate (LTO). NMC and LFP are currently dominating the market in Germany for stationary applications. LTO has a relatively higher life cycle, but due to the comparatively higher cost, they have not been commercialized to much extent [25].

The operating/ambient temperature has a significant effect on battery lifecycle [26]. Higher temperature results in acceleration of battery aging and operational lifetime. The temperatures to achieve best lifetime performance for lithium-ion batteries ranges between 20°to 30°C [27]. In most of the operating regions of WFP with higher ambient temperature, cooling is often necessary.

Containerized Solution:
The battery storage system consists of battery, power management system(PMS) to monitor and estimate power consumption and active operation, power conversion system (PCS) which is responsible for AC/DC conversion through bidirectional inverters, battery management system (BMS) also referred as monitoring and control system which controls individual cell from overcharging and controls charge and discharge of battery. BMS also exchange information and data to communicate with PCS [7]. The entire battery storage system, i.e., battery, PMS, PCS, and BMS can be enclosed within a temperature controlled weatherproof container for the ease of transportation and installation.

The possibilities of integrating lithium-ion battery storage with various variable renewable energy technologies will be studied in section 6.4.

4. Concept Design of Type I Systems

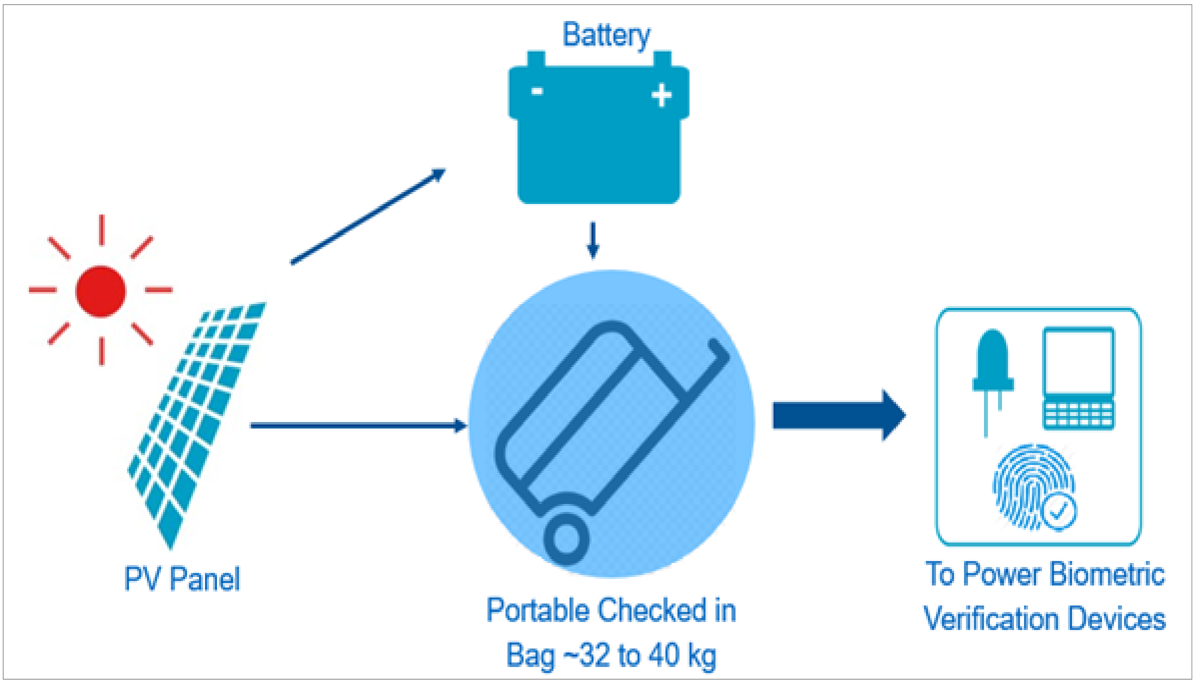

Figure 7: Type I System Concept Design Layout

As already explained in section 2.1.1. WFP is in the requirement of Type I fast response energy supply systems to facilitate WFP team in carrying out biometric verification at the remote location. Since, most of the WFP sites are off-grid, in order to power biometric verification devices, laptops, printers, etc., the total energy demand is 800Wh for a period of 8 hrs. between 9 to 17hrs. The Type I system is designed and analyzed for three different configurations as explained below.

4.1 Analysis and Design of Type I System

As shown in Figure 7, the primary consideration for system design and sizing is such that both battery and PV Panel should be portable as checked baggage with max total weight ranging b/w 32 to 40 kg. The portable Type I system can be designed with three different configurations.

4.1.1 Configuration 1: Sizing Dependent on Battery Storage

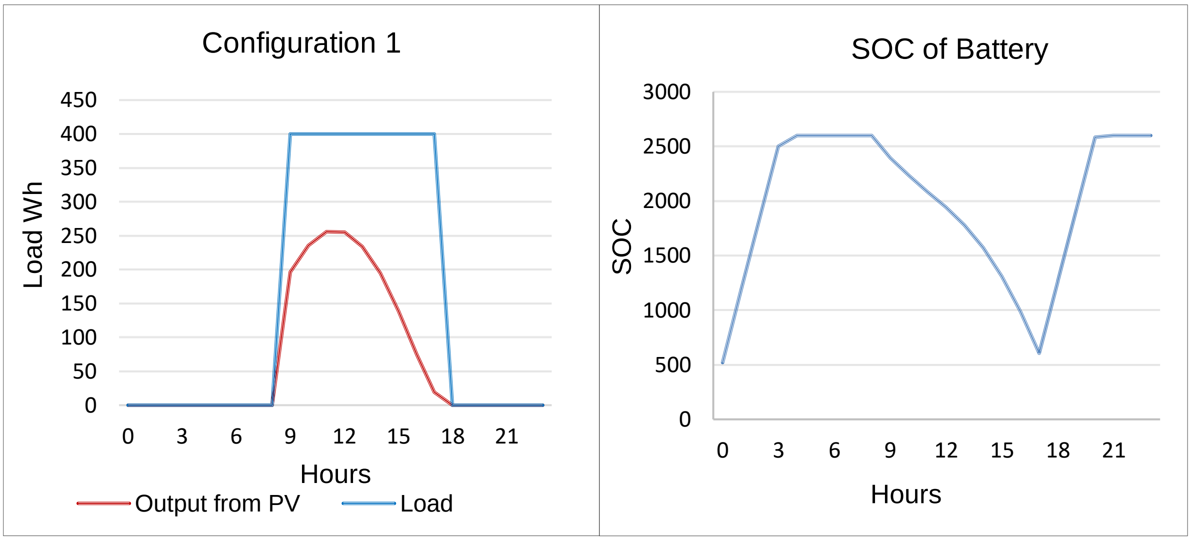

Figure 8: Configuration 1, Load Profile and SOC of Battery

In this configuration, the system is designed such that most of the energy is delivered through battery storage. This will result in a large capacity of the battery and smaller PV capacity.

As we can observe from the above Figure 8, an only small portion of the energy required is delivered by PV panels between 9 to 17 hrs. the balance of which is to be delivered by battery storage. The system was analyzed for the Chad site location, and the optimum sizing of PV panels and storage capacity were calculated. The design parameters calculated are as indicated in the table below.

Table 1: Configuration 1, Type I System Design Parameters

PV Capacity	300Wp
Lithium-Ion Battery Capacity	2600Wh
Minimum SOC	520Wh
Weight, (Panels + Storage)	40kg (10 + 30)

With the above configuration, the battery has to be charged by an external AC source of supply and would take up to four hrs., to charge fully from 20% SOC. Once fully charged, the battery would get discharged during the operating time between 9 to 17hrs. to minimum SOC of 520Wh. Also, it should be noted that we can deliver only 400Wh of energy demand during the operating hours because of the system weight constraint.

4.1.2 Configuration 2: Sizing Dependent on PV Panels

In this configuration, the system is designed such that most of the energy is delivered through solar panels. This will result in a larger capacity of PV panels and reduction in battery storage capacity.

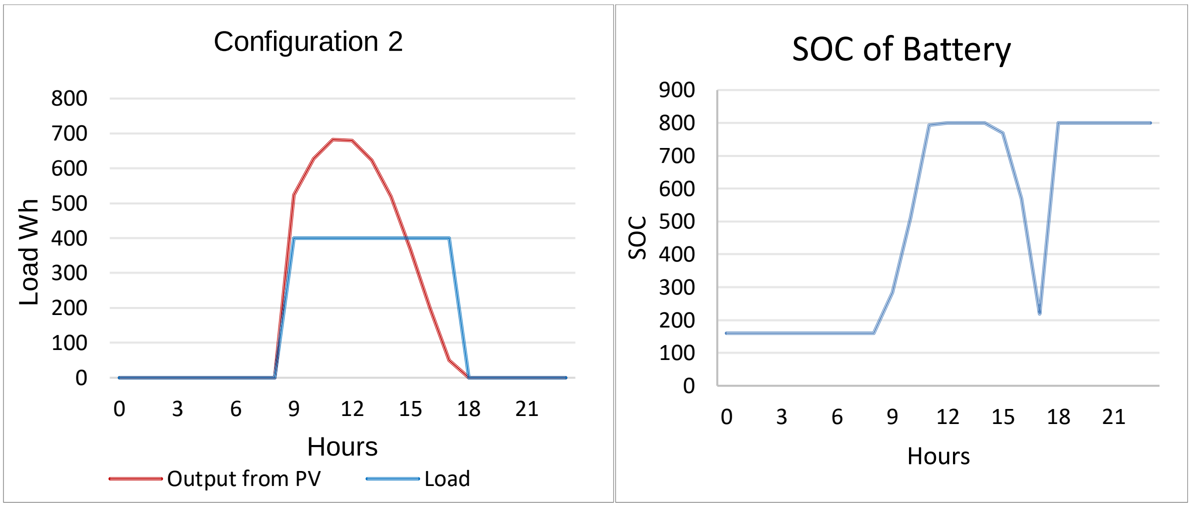

Figure 9: Configuration 2, Load Profile and SOC of Battery

As we can observe from the above Figure 9, most of the energy is delivered by PV panels between 9 to 14 hrs. the balance of which is to be delivered by battery storage between 14 to 17 hrs. The design parameters calculated are as indicated in the table below.

Table 2: Configuration 2, Type I System Design Parameters

PV Capacity	800Wp
Lithium-Ion Battery Capacity	800Wh
Minimum SOC	160Wh
Weight, (Panels + Storage)	41kg (16 + 25)

With the above configuration, the battery gets charged by PV panels between 9 to 14 hrs. and it may take up to 4hrs. to fully recharge depending on solar radiation. Once fully charged, the battery would get discharged between 14 to 17hrs. to minimum SOC of 160Wh. With this configuration, we were able to reduce the battery capacity from 2600Wh to 800Wh.

4.1.3 Configuration 3: Sizing by Restricting Battery Capacity to 100Wh

As per the Federal Aviation Administration (FAA) regulations, it was found that the maximum rating of lithium-ion rechargeable batteries permitted to carry on an aircraft is restricted to 100Wh [28] [29]. Considering weight constraint, configuration 3 has been analyzed.

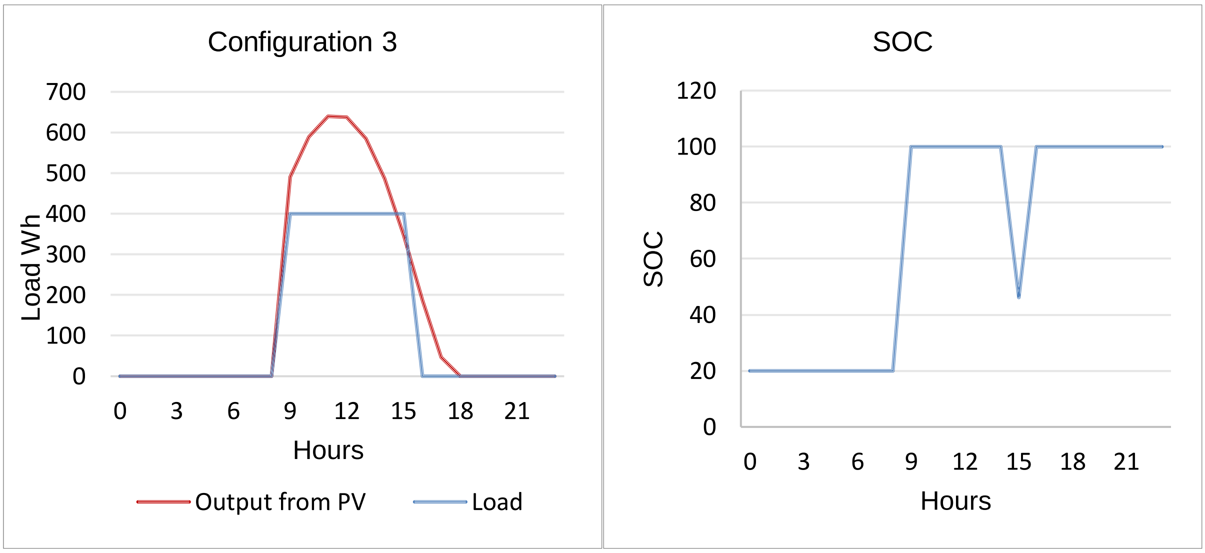

Figure 10: Configuration 3, Load Profile and SOC of Battery

As we can observe from the above Figure 10, most of the energy is delivered by PV panels between 9 to 15hrs. The design parameters calculated are as indicated in the table below.

Table 3: Configuration 3, Type I System Design Parameters

PV Capacity	750Wp
Lithium-Ion Battery Capacity	100Wh
Minimum SOC	20Wh
Weight, (Panels + Storage)	35kg (10 + 25)

With the above configuration, because of the restriction of storage capacity, we can only utilize the system to meet load demands of 400Wh for 6 hrs. i.e., between 9 to 15hrs. However, the advantage is that it can be carried in aircraft as checked baggage as battery capacity is within the specified limit as per aviation travel regulations.

4.2 Prototype

“A prototype is an early sample, model or release of a product built to test a concept or process or to act as a thing to be replicated or learned from” [30]. One such prototype of Type I system was fabricated at UnternehmerTUM MakerSpace Gmbh Garching [31].

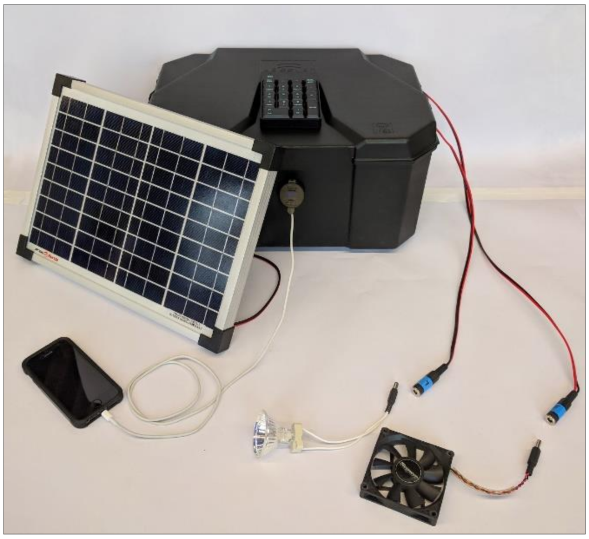

Figure 11: Prototype Model of Type I System, @copyright Denim, Solar Seed

As shown in Figure 11, a small working prototype model was designed and fabricated for demonstration purpose with a panel of 10 W and battery capacity 100Wh including charge controller/inverter, etc.

As per the WFP requirement, the Type I systems can be customized to meet the energy demands considering weight and battery capacity constraints w.r.t travel regulations. It is to be noted that if the system is designed to be dependent on PV panel with minimal battery capacity, then the system cannot be reliable as the output is dependent on solar radiation subjected to variability based on resource location and other site parameters.

5. Concept Design and Site Analysis for Type II System:

As already described in section 2.1.2, most of the WFP offices carrying out humanitarian operations are located in the remote locations where the national grid is unstable or absent [3]. Diesel generators are often used to power facilities in these areas which is expensive and environmental unsustainable way of producing energy. In this section, we will try to analyze the possibility of installing a microgrid hybrid renewable system at one of such WFP site location by evaluating various available natural resources such as wind, solar, micro-hydro, etc. along with understanding the load profile.

5.1 Microgrid Concept

Microgrids are considered to be one of the most promising solutions to integrate decentralized renewable energy generation into electric power system [5].

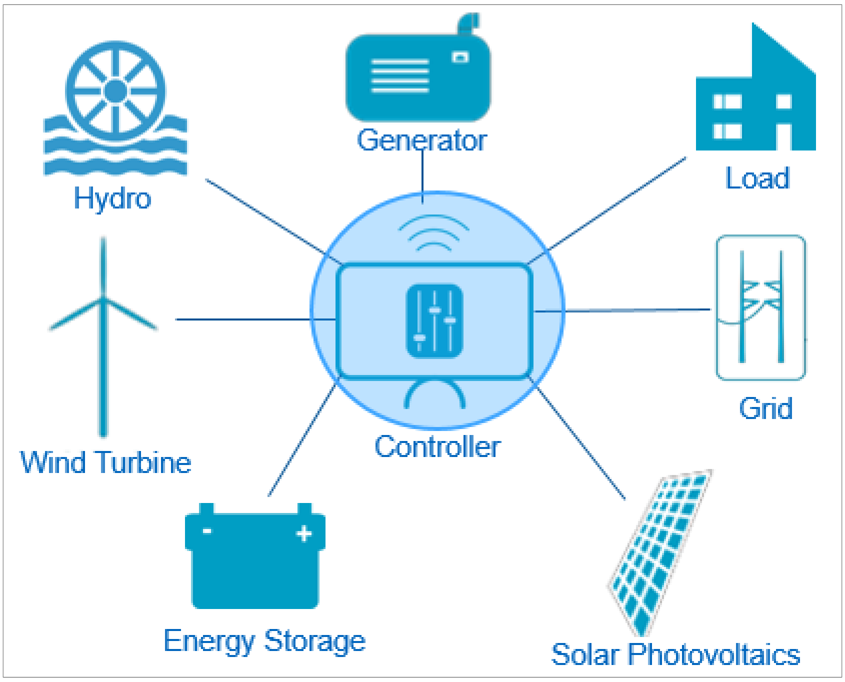

Figure 12: Microgrid Schematic

As per CORDIS Europe (Community Research and Development Information Service), “Microgrids are defined as a series of electrical loads, elements of generated power supply (wind, photovoltaic, microturbine, etc.) and storage elements (batteries, compressed air, etc.) which, connected to the electric grid by means of a single point of connection, are all linked through a strategy which manages both the flow of energy within the grid as well as the interchange of power with the general supply grid” [32].

The microgrid controller is responsible for the satisfactory automated operation and control of microgrid working either in islanded or grid-connected mode [33]. The control algorithm that will be adopted in my simulation study is Cycle Charging. Under Cycle Charging, whenever the generator is turned on automatically, it operates at full capacity (i.e., at best efficiency point) to meet the load demand, and the surplus power charges the battery bank till the battery reaches SOC of 80% [34].

5.1.1 Microgrid Layouts

The economic viability of the project is dependent on the proper selection of microgrid architecture. The microgrid architecture can be based on AC busses or DC busses, or combination of both, i.e., hybrid AC-DC microgrid and other groups can include DC zonal microgrid, a solid-state transformer based microgrid, etc. AC microgrid can be a most suitable option for the existing system with AC loads because of the requirement of minimum modification on the existing installation. DC microgrids with better performance can be considered for new installations [35].

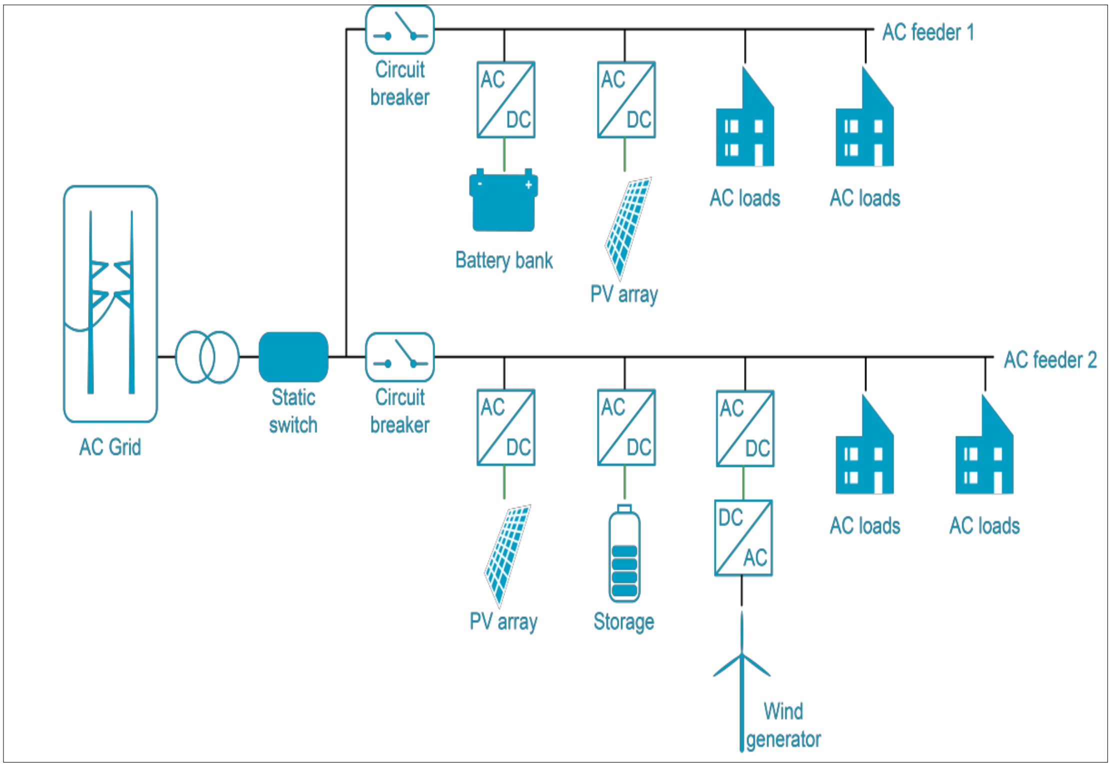

Figure 13: AC Microgrid Architecture **[35]**

The AC microgrids consist of transformers, static switch, PCC (Point of common coupling) along with many AC/DC or D/AC converters as shown in Figure 13. Circuit breakers manage the interconnection of the distributed generators, the loads and the grid. At the PCC, the main circuit breaker, i.e., the static switch is placed that manages grid connected operating mode, islanded mode and the transition between both operating modes. AC microgrid architecture operating in grid-connected mode provides higher reliability as the power flows directly from grid avoiding any series connected converter. The voltage and frequency of the feeders remain same as the grid. However, at most of the WFP office location the grid is unstable or of poor quality with frequent and significant voltage fluctuations, even over 25% and frequency fluctuations >=10%. Hence, stabilizers are very much required to prevent equipment being damaged by unstable grid voltage. The main disadvantage of AC microgrid is the complex power converters leading to an increased power loss and a decrease in reliability [36], [35], [37].

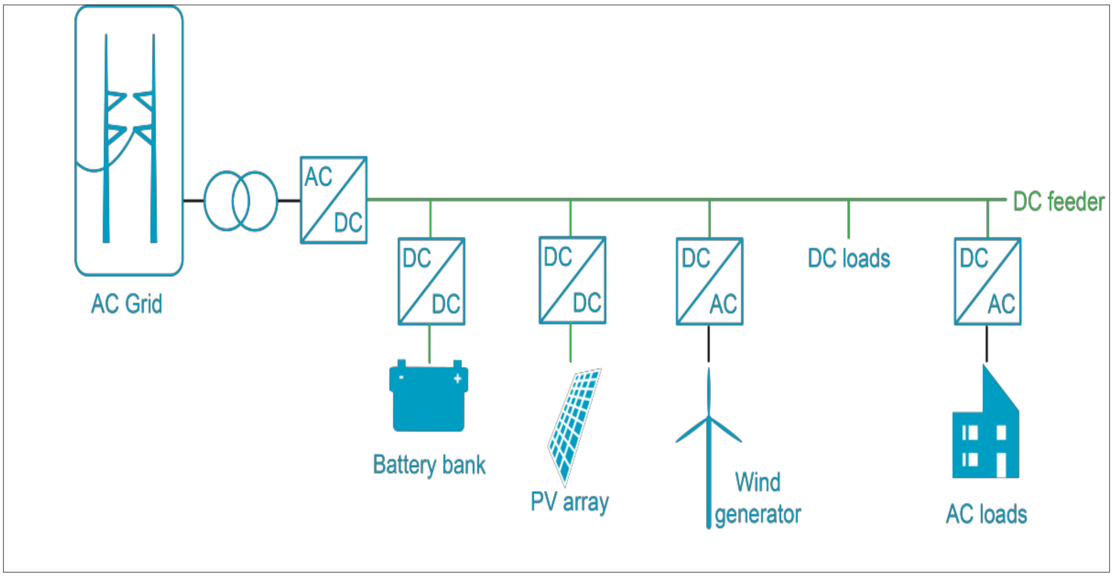

Figure 14: DC Microgrid Architecture **[35]**

The DC microgrid is connected to the grid through an AC/DC converter which regulates the voltage of DC bus as shown in Figure 14. The AC loads are connected to the DC bus using DC/AC converter. DC loads can sometimes be connected directly to the DC bus or may need D/DC converters depending on DC bus voltage. The main advantage of DC microgrid architecture is the reduced number of converters/rectifiers compared to AC microgrid. The main disadvantage is the reduced reliability due to the series connected bidirectional AC/DC converter controlling the power flow from/to the distribution grid [35], [37].

5.2 Site Survey

5.2.1 Site Location

Out of more than 1100 WFP office locations, I have chosen WFP office Jalalabad situated in Afghanistan for my analysis, which is one of WFP's next target location to analyze and install a renewable hybrid system to reduce operating cost and environmental impact because of CO_2 emissions from diesel generators.

In Afghanistan, about 60% of the total electricity demand is met by importing energy from neighboring countries, i.e., Uzbekistan, Tajikistan, Turkmenistan, and Iran. Local production includes 44% of hydropower power plants, 41% of thermal power plants and 15 % of diesel generators. Less than 11% of rural population has access to grid electricity, whereas, in large urban areas including cities like Kabul, Kandahar, Herat, and Mazar-e-Sharif, more than 90% of the population has access to electricity from grid [38].

Jalalabad city is located in eastern Afghanistan at the junction of Kabul and Kunar river. It is approximately 130km east to Peshawar city of Pakistan. It covers a land area of 122km^2 with a population of 360000 people [39].

Figure 15: Afghanistan Map and Jalalabad WFP Office Snapshot from Google Maps

From the google maps image above in Figure 15, we can observe that WFP Jalalabad office is located close to the Jalalabad Airport and is at a distance of approx.1.04 km away from Kabul River.

5.2.2 WFP Jalalabad Office Overview

After having discussions with WFP team and analyzing WFP Jalalabad office site survey report [11], data were collected to understand the electricity load profile, generator fuel consumption, and other site-related parameters required for my analysis.

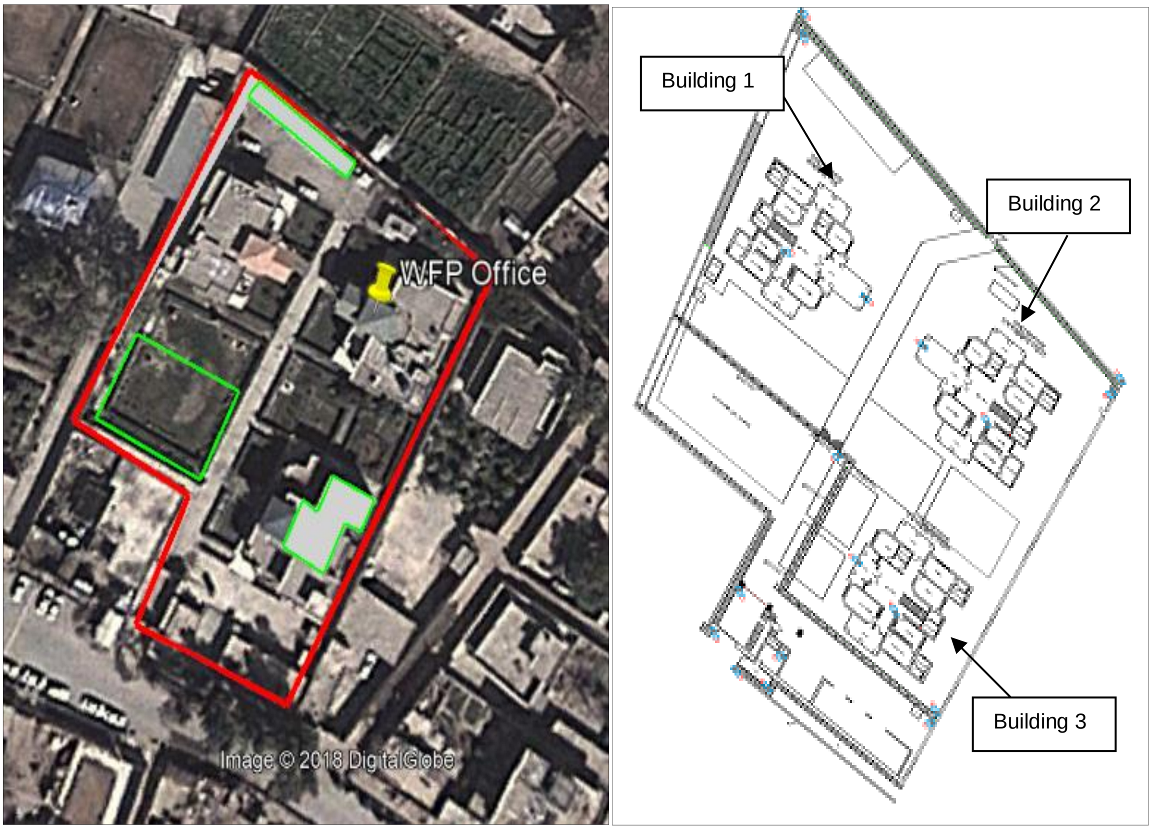

Figure 16: Google Satellite Image of WFP Office Jalalabad (Left), Office Floor Plan (Right)

The office is situated on the outskirts of a residential area in the north-west of Jalalabad with coordinates 34°25'45.44"N, 70°28'19.95"E. The red outline in the above Figure 16 indicates the WFP office compound which covers an area 5800m^2 and the area covered by green outline indicates the available free space for installation of PV panels which estimates to around 60kW of PV capacity. The compounds have three large main two-story building as we can observe in the floor plan figure above. The office currently has approximately 30 WFP staff on site along with 23 supporting staff [11].

5.3 Load Data

As already explained about “Green Kit” (an energy monitoring system) in section 2.2, an energy monitor was installed at Jalalabad office. However, as mentioned in WFP site survey report it was found that the monitoring system was set to 120V, 60Hz instead of 230V, 50Hz which the office is operating on. This resulted in showing only half of the actual energy consumption by the monitoring system. Additionally, the monitoring system was not connected to the distribution board of all the three building within the compound resulting in showing the energy consumption of only one building [11].

Based on the survey data available, energy consumption based on the installed electrical appliances at the site was approximated to 630 kWh/day with a peak power demand of 90kW. Considering all the discrepancies observed in the monitored data, the hourly load data obtained through monitoring system was scaled to match the average consumption of 630kWh/day.

5.3.1 Load Profile

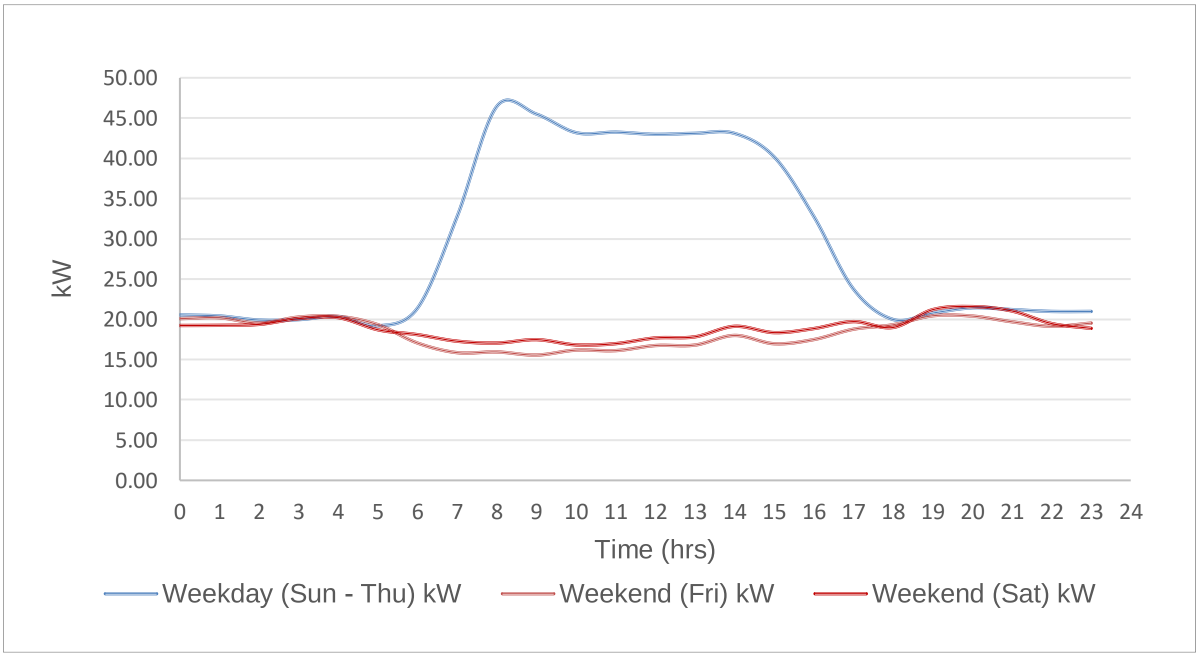

Figure 17: Average Hourly Load Profile

The average hourly load profile was calculated after analyzing and scaling the load data available for 8760hrs from the period between 1st Jan 2017 to 31st Dec 2017. As we can observe from the above figure, the energy demand is maximum during the office timings on a weekday, i.e., between 8 to 16hrs. Being an Islamic country, the weekend is on Friday and Saturday during which the average hourly load demand is below 20kW.

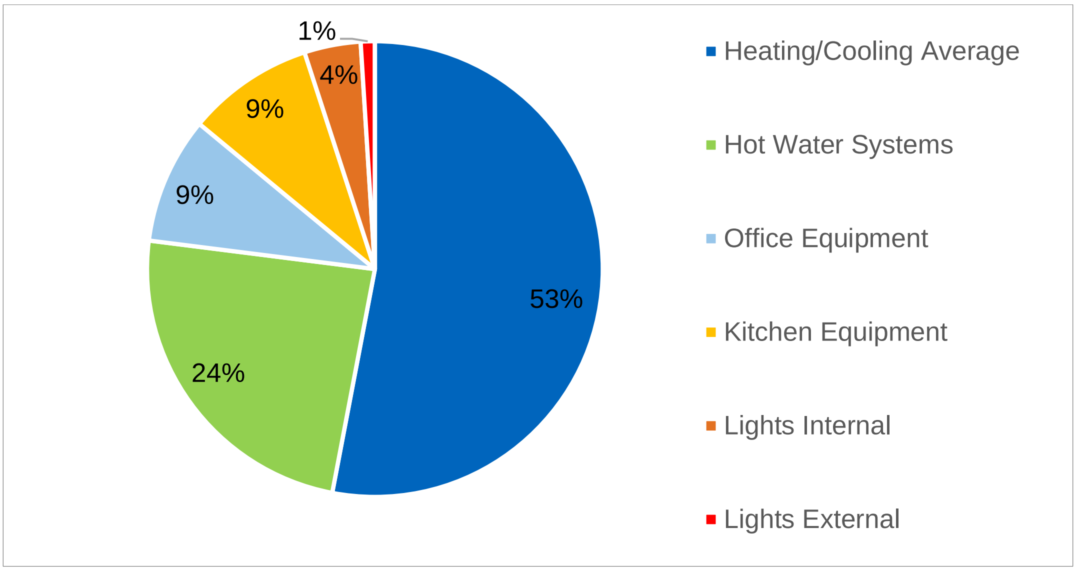

Figure 18: Electrical Consumption of different Appliances

Figure 18 above shows the distribution of energy consumption of different appliance contributing to the total load demand of 630kWh/day. As we can observe, more than 75% of the total demand constitutes from the operation of air-conditioning during summer, and heat pumps and hot water systems during winter.

5.3.2 Monthly Fluctuation of Load and Temperature Profile:

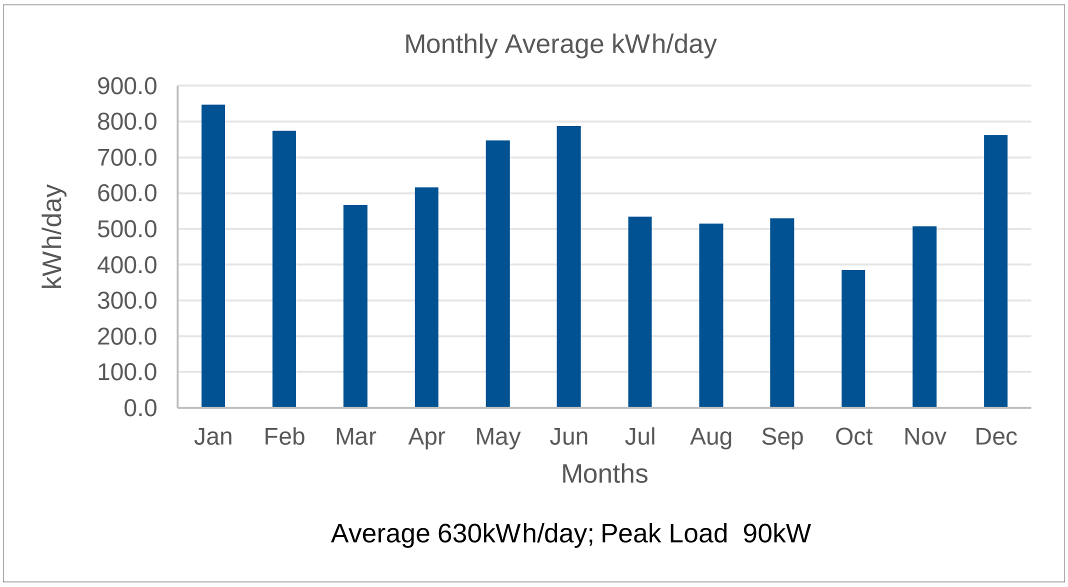

Figure 19: Monthly Average Daily Load Consumption

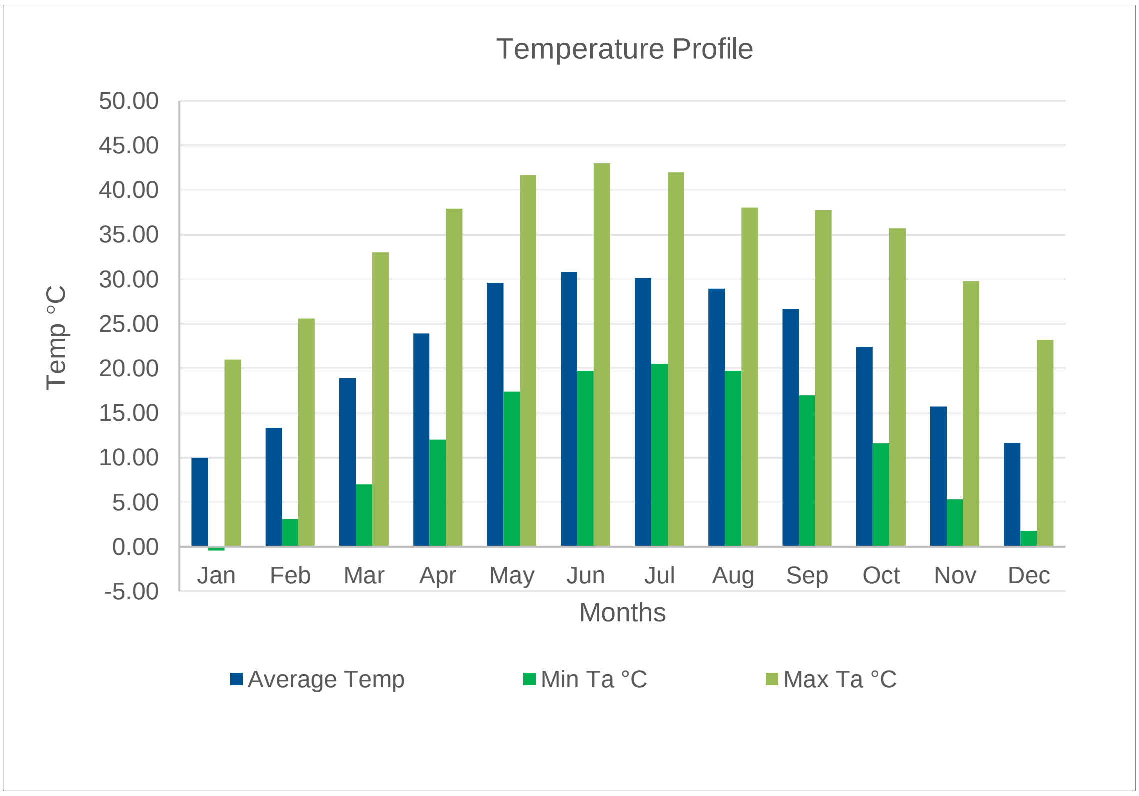

Figure 20: Temperature Profile of Jalalabad

Figure 19 and Figure 20 above shows the monthly fluctuation of load and temperature profile. We can observe that during the summer and winter season the load demands are higher due to cooling and heating loads respectively when compared to other seasons. The temperature profile was plotted with data obtained through Meteonorm [40].

5.4 Solar Radiation Analysis for the site

5.4.1 Sun Path: Elevation vs. Azimuth Angle

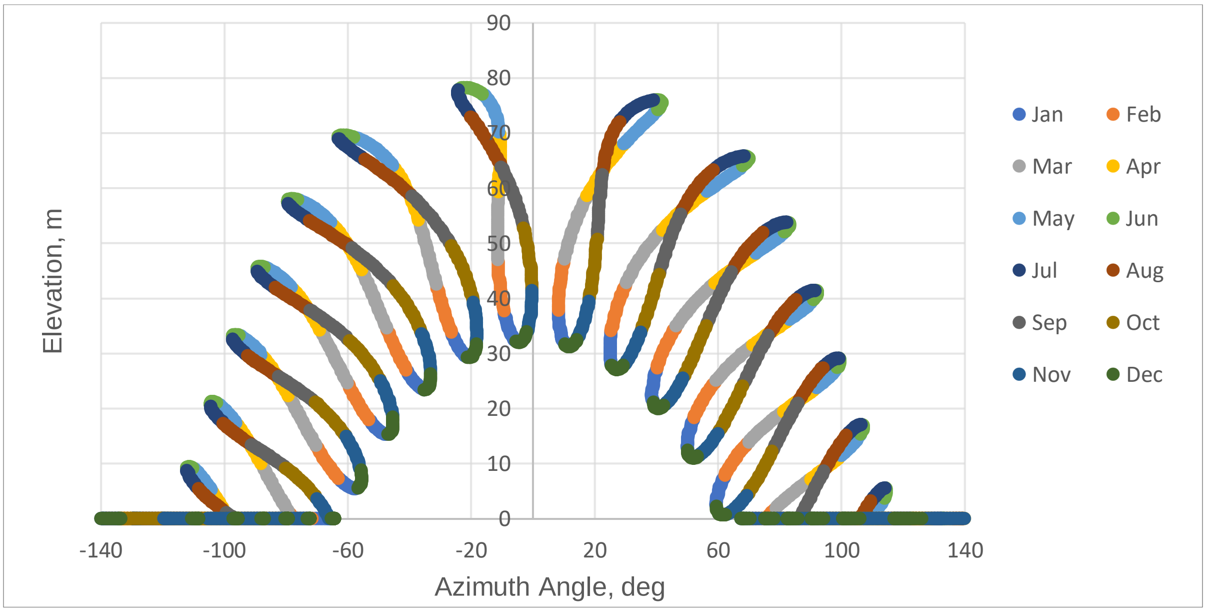

Figure 21: Sun Path at Jalalabad

Hourly solar data was extracted from Meteonorm [40]. The Figure 21 above was plotted showing the suns path for different months with the change in elevation and azimuth angles. We can observe that sun is at the highest position during summer, i.e., the month of June and at the lowest position during the winter season.

5.4.2 Monthly Solar Radiation Profile

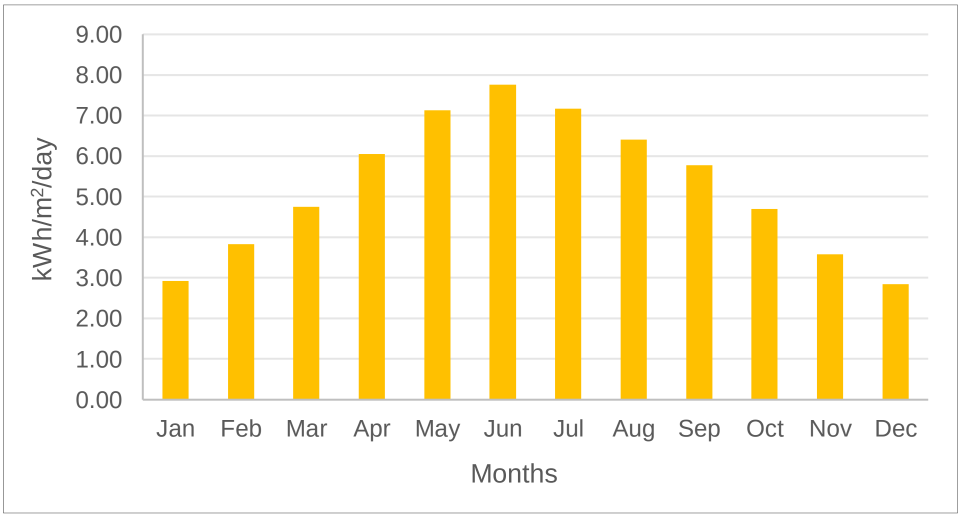

Figure 22: Daily Solar Radiation (Global Horizontal)

Figure 22 above shows monthly global horizontal irradiance. The average daily solar radiation calculated for Jalalabad is 5.24 kWh/m^2/day.

5.4.3 Solar Module Tilt Angle

a) Optimum Tilt Angle

The panel optimum tilt angle is an important parameter which influences the amount of solar radiation falling on the panel surface. The optimum tilt angle can be calculated based on position of sun, attitude and local geographical characteristics [41] [42].

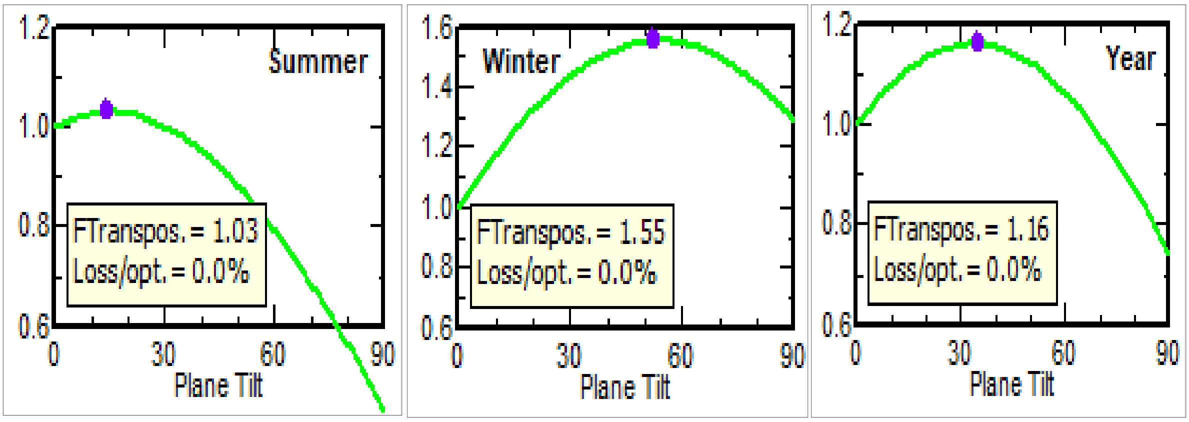

Figure 23: Optimum Panel Tilt Angle for Summer, Winter and Year

The Figure 23 above shows optimum tilt angle for solar panel for summer and winter season [43]. However, since the panels are fixed without tracking, the yearly tilt angle to achieve minimum losses was calculated to be 35°.

Table 4: Optimum Tilt angle and Losses

Seasons	Optimum Tilt Angle	Losses		
		Summer Loss	Winter Loss	Yearly Loss
Summer (Apr. to Sep.)	14°	0	-20.1%	-4.8%
Winter (Oct. to Mar.)	52°	-15.8%	0	-4.1%
Yearly	35°	-4.8%	-4.6%	0

Considering the PV panels with fixed tilt, the table above summarizes the optimum tilt angle required for different season and the corresponding energy losses in the other seasons [43].

b) Effect of Tilt Angle on Panel Row Spacing

The module tilt angle and spacing determines the peak power that can be produced and also the maximum solar energy that can be absorbed. One method is to orient the panel to the optimum tilt angle and have sufficient row spacing between panel to avoid shading. This will result in a smaller system because of empty space between each panel row. The second approach can be to mount the modules close to each other with reduced tilt which results in much larger peak capacity but results in less productivity from each module [23]. As analyzed in many literature studies, if the roof area is fixed or constrained then the economic benefit can be maximized at a relatively lower tilt angle and high GCR (Ground Clearance Ratio). GCR is the ratio of total PV area divided by ground/roof area where PV is installed. With the higher tilt angle, the ground area required increases to avoid interrow shading which results in lower GCR when compared to lower tilt angle [44].

The analysis was carried out to understand the interrow spacing required and the effect of zero tilt for our system in Jalalabad.

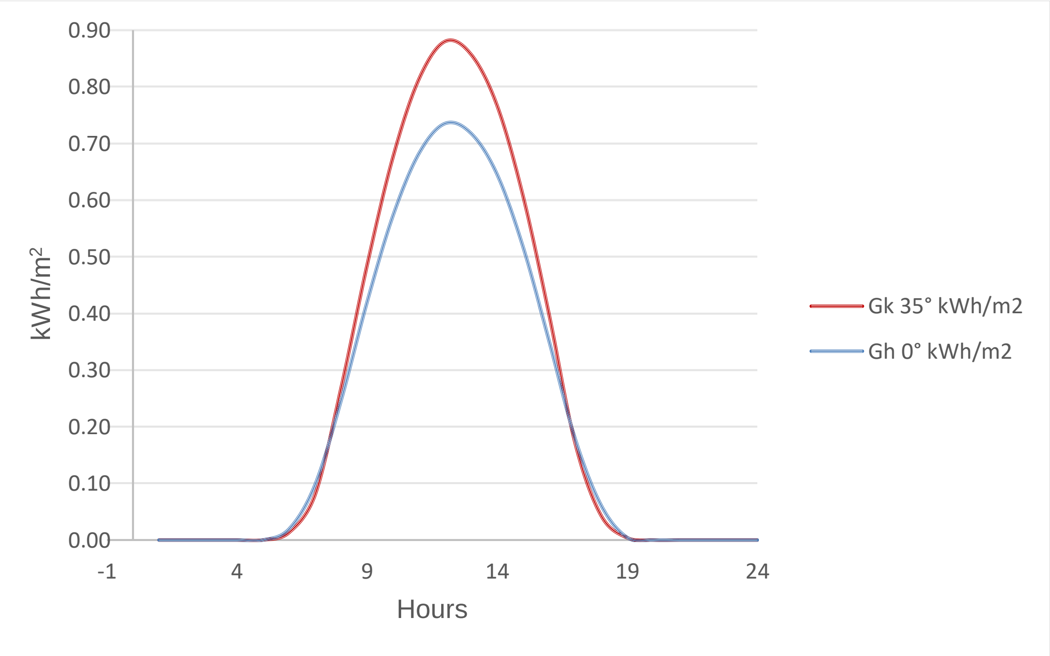

Figure 24: Variation of Solar Radiation with and without Tilt

Figure 24 above shows average hourly radiation with optimum tilt (i.e., 35°) and with zero tilt angle of the panel. It was calculated that with zero tilt angle, we face yearly radiation loss of -13.8%, winter and summer season energy loss of -35.6% and -2.5% respectively.

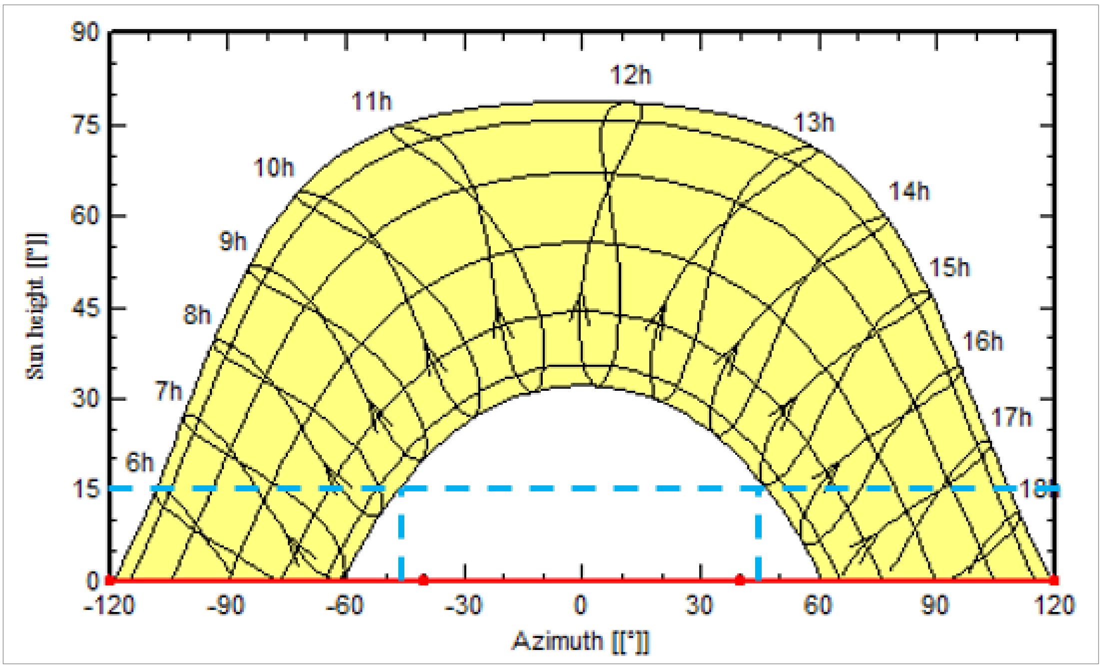

Figure 25: Sun Path to Determine Inter Row Shading

Figure 25 from PVsyst [43] was used to determine the inter-row shading of panels at an optimum tilt angle of 35° facing south. Considering winter solstice from 8.30 am to 3 pm for the worst-case scenario when the sun is at the lowest angle having narrowest range of azimuth angles [45], we can calculate from above figure the sun height and azimuth as 15°and 45° respectively. Considering each module as 330Wp (model number CS6U-340M from Canadian solar) with the module width of 990mm, the row spacing required to avoid inter-row shading of panels was calculated to be 1.5m. The row spacing can be reduced to 1m if we reduce the winter solstice timing from 10 am to 2 pm.

Analysis was also conducted in HelioScope software [46] to determine if the available roof/free area of WFP office (as indicated in WFP site survey report, Figure 16) was sufficient to install 60kWp of PV panels with optimum tilt of 35° considering row spacing for winter solstice timing from 10 am to 2 pm.

Figure 26: PV Panel Layout Design with 10° Tilt facing South at WFP Office Jalalabad

Preliminary analysis showed that the available roof area at the site might not be sufficient to install 60kW of solar but rather possible to install only up to 40kW. Hence, in order to install 60kWp, the tilt angle has to be reduced to 10° (i.e., close to optimum tilt angle for summer) or site survey has to be carried out to check the possibility for additional space available. Figure 26 shows the PV panel layout designed at 10° panel tilt.

However, during detail design stage further analysis should be carried out prior to installation, after approval of final layout of available site area. Accordingly, the best decision shall be made based on final techno-economic analysis considering parameters discussed above.

5.5 Wind Analysis for Site

The energy that can be extracted from the wind varies as the cube of the wind speed. Hence it is important to understand the characteristics of wind resource for wind energy exploitation, in terms of identification of suitable sites and prediction of economic viability [16].

The wind data was extracted from NASA surface meteorology and solar energy database. The wind speed data is for 50m above the surface of the earth for the terrain, monthly averaged over the 10year period.

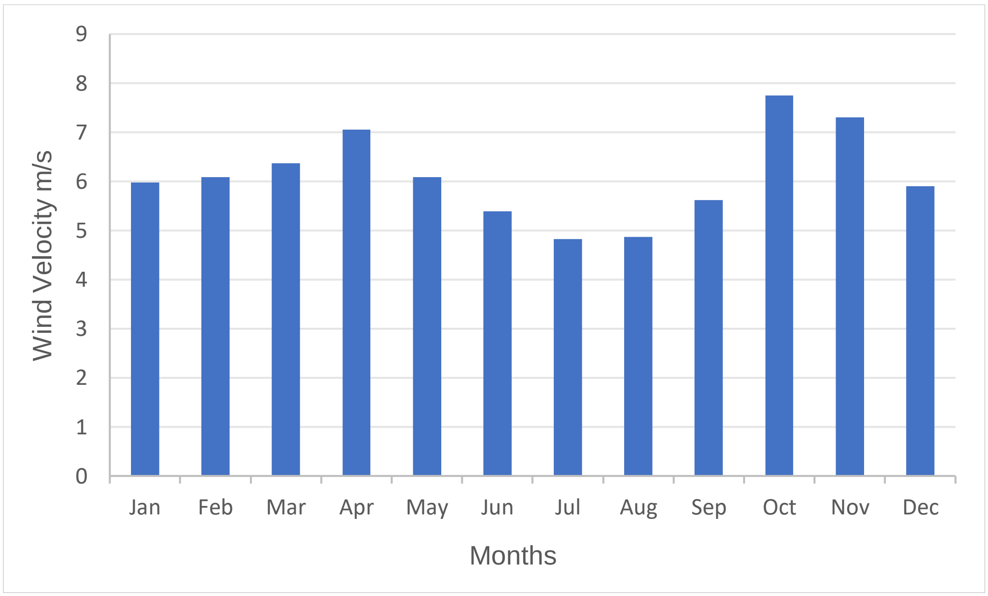

Figure 27: Average Wind Velocity @ 50m Hub Height

The Figure 27 above shows the monthly fluctuation of wind speed. The average wind velocity is approximately 6 m/s for Jalalabad site at 50m hub height.

5.5.1 Weibull Distribution Curve

One of the characteristics of wind is variability, both geographically and temporally. The Weibull distribution is often used to characterize the variation in hourly mean wind speed over a year at many typical sites. The distribution can be mathematically represented as

$$\mathrm{F(U)} = \exp(-\left(\frac{U}{c}\right)^{k}) \tag{1}$$

Where F(U) is the fraction of time for which hourly mean wind speed exceeds U. It is characterized by two parameters: a ‘scale parameter’ c and a ‘shape parameter’ k which describes the variability about the mean [16].

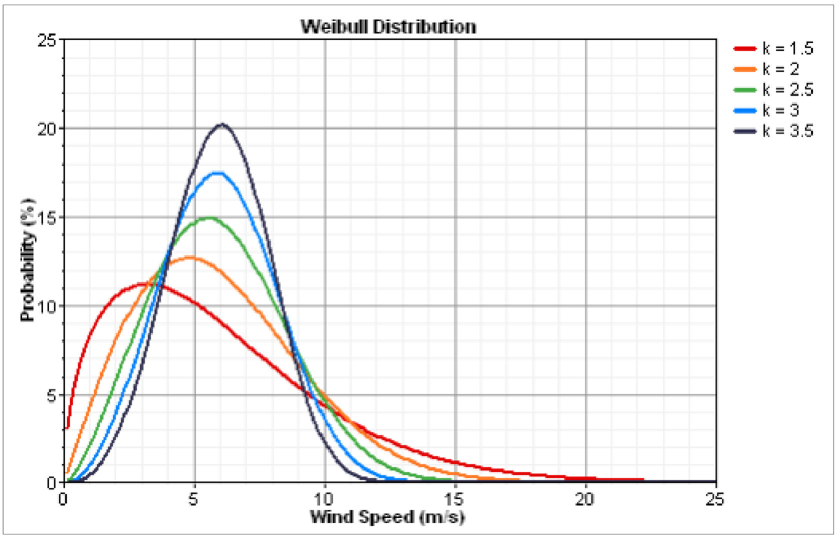

Figure 28: Weibull Distribution Curve at Average Wind Speed of 6 m/s

Figure 28 above shows the Weibull distribution for an average wind speed of 6m/s with different Weibull k value. The scale ‘c’ and shape factor ‘k’ determines the breadth of distribution of wind speed. As we can observe in the graph, higher k values correspond to narrow distribution of wind speed, and lower k values correspond to broader wind speed distribution. Hence, a location with steady wind speed will have higher k value (3 or 4), whereas the site with gust wind will have lower k values (1.5 or 1.2) [34].

These variations are also driven by changes in isolation during the year as a result of the tilt of the earth’s axis of rotation. For our analysis, k value of 2 is considered, which is typical for many locations [16].

5.6 Micro-Hydro River Flow Analysis

Micro-Hydro also known as hydrokinetic turbines placed within a free-flowing river water stream capture the kinetic energy of water to generate power. Flowing water resources with little or no elevation can be harnessed by hydrokinetic energy conversion system. The energy generated by these turbines varies with the river flow velocity with the maximum energy generated with higher water flow velocity. “Hydrokinetic technology is considered as a cheap and best suitable alternative to supply electricity in remote and off-grid areas” [19], [47].

WFP Jalalabad office is located approximately 1.04km away from Kabul river as shown in Figure 15. In this section, we will analyze the Kabul river flow path and the seasonal fluctuation of flow velocity to harness energy from the water stream using hydrokinetic turbines.

5.6.1 Kabul River Flow Path in Jalalabad

The Kabul River rises in the Sanglakh Range in the Hindu Kush (the mountain range that stretches near the Afghan-Pakistan border), 72km west of Kabul. It is approximately 700 km long, and for 560km its trajectory carries it through Afghanistan. It flows east through Afghanistan's capital Kabul and then the city of Jalalabad, before crossing the border into Pakistan [48] [49] [50].

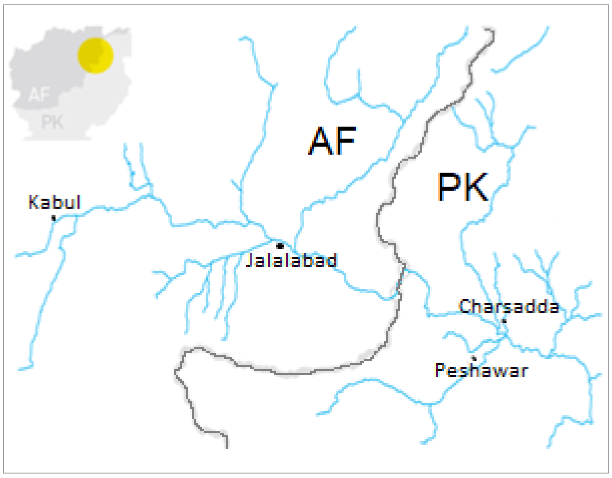

Figure 29: Kabul River Flow Path **[48]**

Figure 29, shows the map of Kabul river flowing through Jalalabad in Afghanistan(AF) and entering into Pakistan (PK).

5.6.2 Percentage Monthly Water Discharge and River Flow Velocities

To analyze the monthly water discharge. Through literature reviews, it was possible to extract some data from the hydrological stations located in Jalalabad.

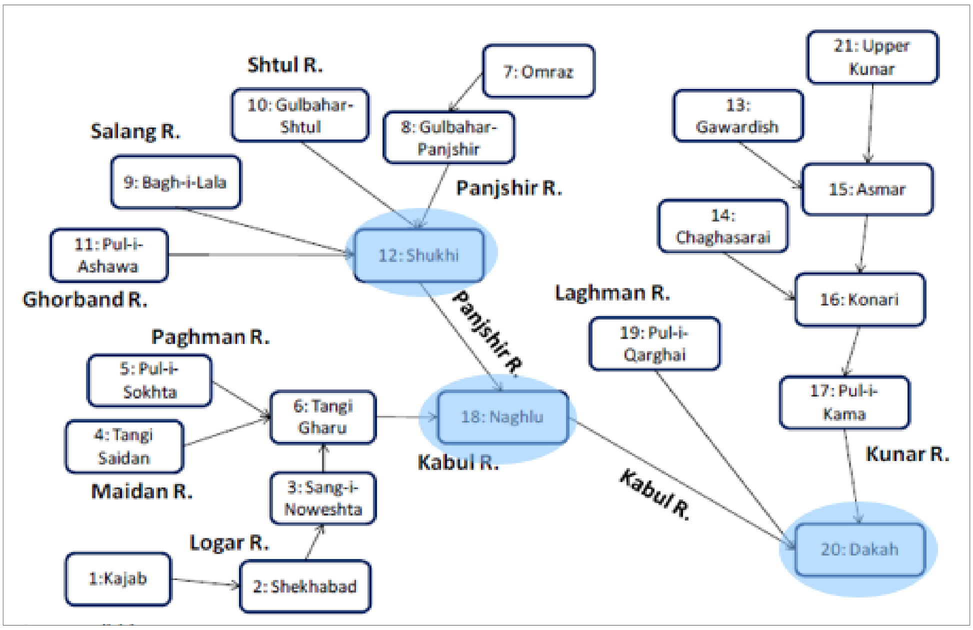

Figure 30: Hydrological Stations at Jalalabad **[51]**

Figure 30 shows hydrological stations at Jalalabad. My studies focused on the hydrological stations Shukhi and Dakah where the Kabul river flow discharge data was recorded [51].

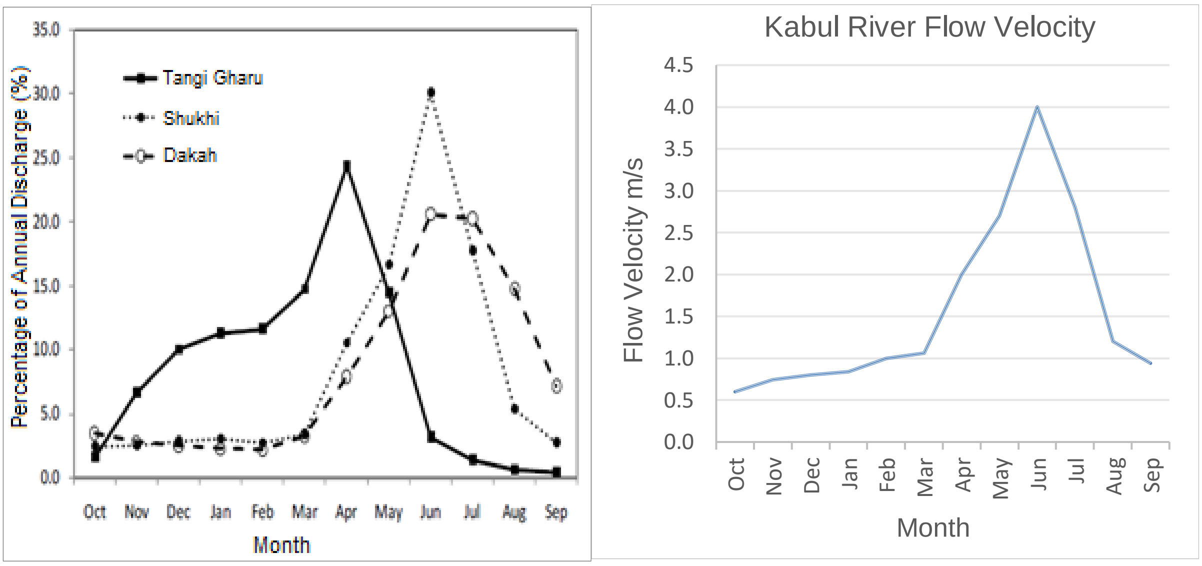

Figure 31: Percentage Discharge and Monthly Kabul River Flow Velocity

As we can observe in Figure 31, at the Shukhi station in the Panjshir sub-basin, the peak discharge appears in June; the minimum appears during winter. The monthly variation of discharge is strongly affected by snow accumulation and its melting process with the temperature being highest in summer season and lowest during winter. A similar pattern is observed at Dakah station. The depth of runoff at Naghlu and Dakah station is 129mm and 281.5mm respectively [51], [52].

The river flow velocities were approximated accordingly, to match the discharge pattern at Shukhi station. The maximum flow velocity is achieved in the month of June. During the summer season, i.e., April to September, the flow velocity varies between 1.5 to 4m/s, and during the winter season it is below 1m/s, and hence it is not possible to harness energy from the microturbine during the winter season.

Actual river flow velocity measurement at the site should be carried out to validate the approximated results before installation of such microturbines.

6. Modeling and Simulation Study for Type II System:

In this chapter, we will perform modeling and simulation study considering both as off-grid and on-grid system for various scenarios. In on-grid system analysis, we will analyze the existing system at WFP office Jalalabad (i.e., connected to the unreliable grid) and conduct simulations to find the best configuration of the renewable hybrid system to achieve economic savings and reduction of diesel generator fuel consumption and CO_2 emissions.

6.1 Homer Pro Simulation Software

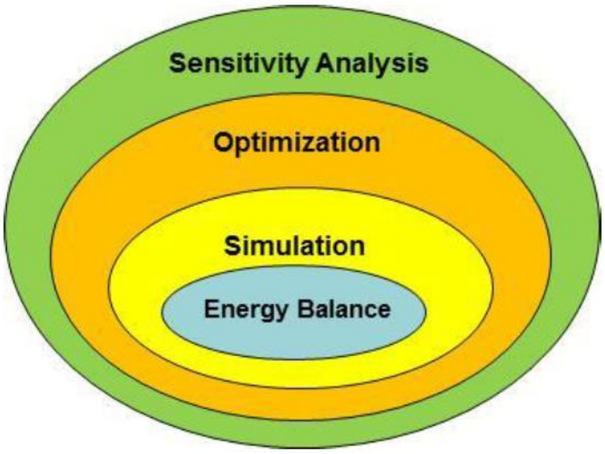

Figure 32: Homer Pro Simulation - Optimization- Sensitivity Analysis Tool **[34]**

The HOMER Pro® microgrid software by HOMER Energy is the trusted global standard for optimizing microgrid design in all sectors. Developed by Department of Energy's National Renewable Energy Laboratory (NREL) in 1992 and privatized in 2009. The HOMER simulation performs an energy balance for each timestep of the year to determine how a particular system is expected to operate for the project lifetime along with economic optimization by determining the least cost option based on lowest net present cost [34].

6.2 Steps in Micro Grid Simulation

The flow diagram in Figure 33 shows the steps that I have followed to conduct the simulation study of microgrid system for WFP office Jalalabad. As we can observe in flow diagram, the initial two steps, i.e., site survey and load profile analysis has already been discussed in chapter 5 of this thesis report.

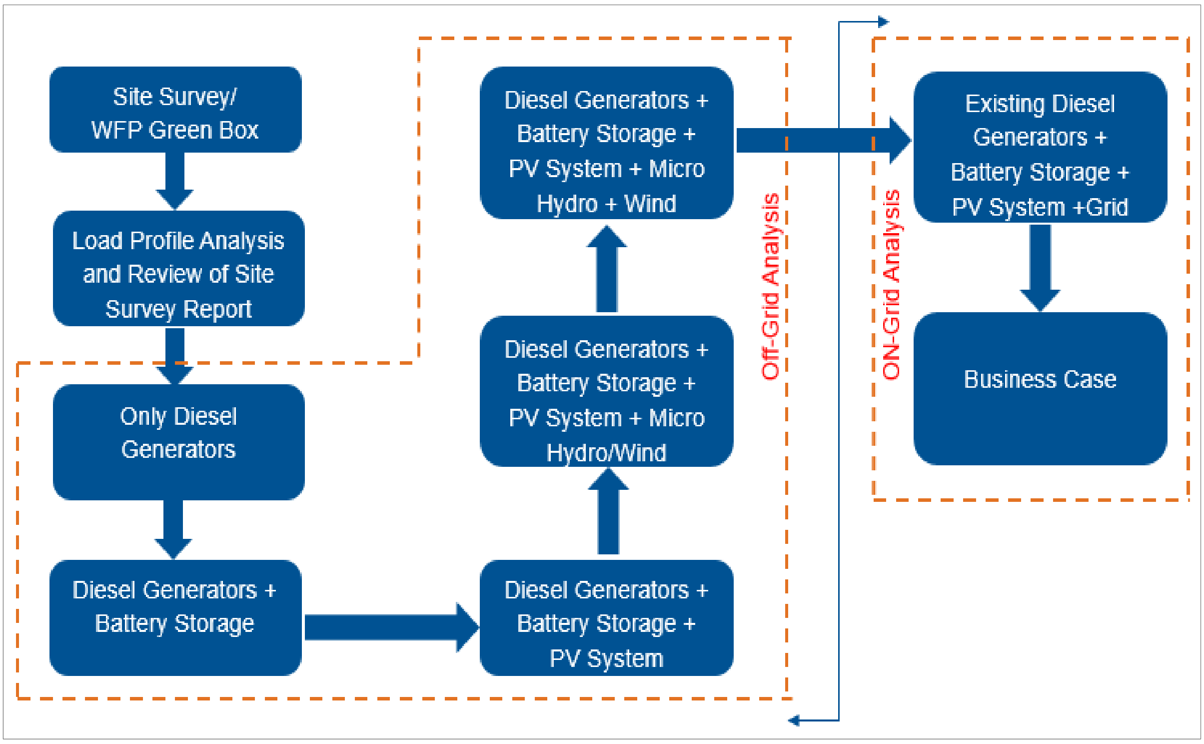

Figure 33: Flow Diagram Showing Steps in Micro Grid Simulation

6.3 Input Parameters for Analysis

The input parameters considered for my analysis is as indicated in the table below.

Table 5: Input Parameters for Simulation Study

Component	Capital/ Replacement Cost	O & M Cost per kW
PV	USD 2600/kW	USD 10/year
Converter	USD 330/kW	USD 0
New Generators	USD 470/kW	USD 0.020/op.hr
Lithium-Ion battery	USD 800/kW	USD 10/year
Existing Generators (No Capital cost, only replacement cost)	USD 470/kW	USD 0.020/op.hr
Micro Hydro 5kW	USD 170000/kW	USD 10/year
Wind	USD 7000/kW	USD 70/year
Other miscellaneous	USD 5000	

Other Parameters	
Project Lifetime	25 years
Diesel Fuel Price	USD 0.67/liter
Discount Rate	4%
Inflation Rate	2%
Generator Life Cycle	15000 hrs.
Max PV Capacity	60kW (due to available space constraints)

The input parameters as indicated in Table 5 have been finalized after discussion with WFP team Rome. Some of the cost parameters, i.e., capital and O&M (operation and maintenance) were also analyzed through literature reviews [53]. All the analysis has been performed considering project lifetime of 25 years. It should be noted that for my analysis, no capital cost is considered for existing generators running at WFP office Jalalabad.

The table below describes the icons that will be included in my analysis results.

Table 6: Description of Simulation Study Icons

Icons	Description
	Renewable Fraction
	LCOE
	Initial Capital
	O & M Cost
	Fuel Cost
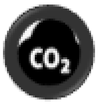	CO_2 Emissions
	Discounted Payback Period

6.4 Off-Grid System Analysis

As already indicated in flow diagram Figure 33, in this subsection we analyze the system considering as completely off-grid, i.e., having no access to national gird.

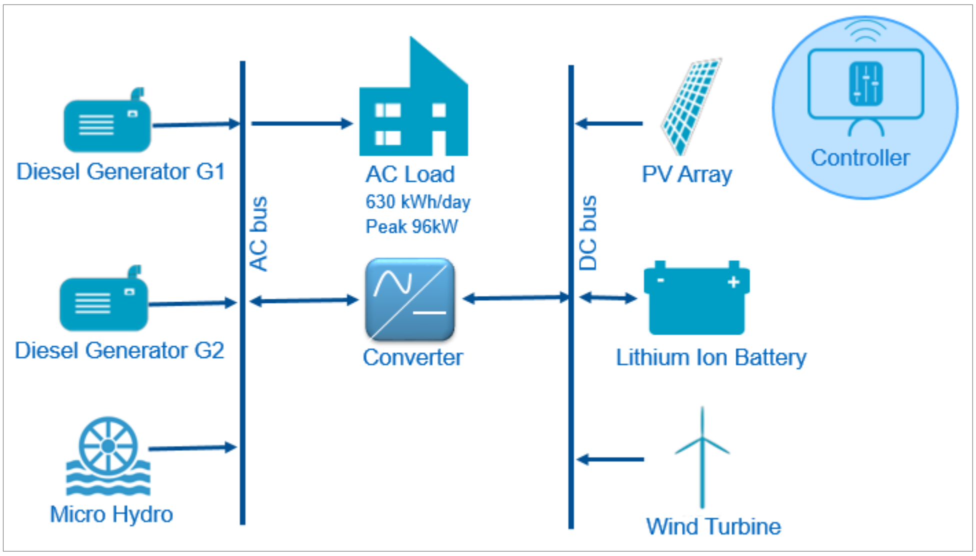

Figure 34: Layout of Off-Grid Hybrid Microgrid System

Figure 34 above shows the final layout of the off-grid system. In the sections below, we will analyze the system step by step by initially considering the system running with only diesel generators and then subsequently adding storage, PV, wind, and micro-hydro and compare the system output profile and savings achieved in each scenario.

6.4.1 Large Diesel Generator (DG)

The amount of fuel the generator consumes to produce electricity is described as fuel curve. The linear function is used in the model. A linear regression technique is used for more than two points to calculate the line of best fit. The equation below gives the generator fuel consumption in units/hr. as a function of its electrical output [34].

$$F = F_0 . Y_{gen} + F_1 . P_{gen} \tag{2}$$

Where,
F_0 = the fuel curve intercept coefficient [units/hr/kW]
F_1 = the fuel curve slope [units/hr/kW]
Y_{gen} = rated capacity of the generator [kW]
P_{gen} = the electrical output of the generator [kW]

The generator’s electrical efficiency as the electrical energy coming out divided by the chemical energy of the fuel going in. The equation below describes the relationship

$$\eta_{gen} = \frac{3.6 \, . \, P_{gen}}{\dot{m}_{fuel} \, . \, LHV_{fuel}} \tag{3}$$

Where,
P_{gen} = the electrical output [kW]
$\dot{m}_{fuel}$ = the mass flow rate of the fuel [kg/hr.]
LHV_{fuel} = the lower heating value (a measure of energy content) of the fuel [MJ/kg]
The factor of 3.6 arises because 1 kWh = 3.6 MJ.

The simulation was performed to determine the optimal sizing of the generator. It was found that in order to match the hourly load profile and peak load, we would require a minimum diesel generator capacity of 110kW.

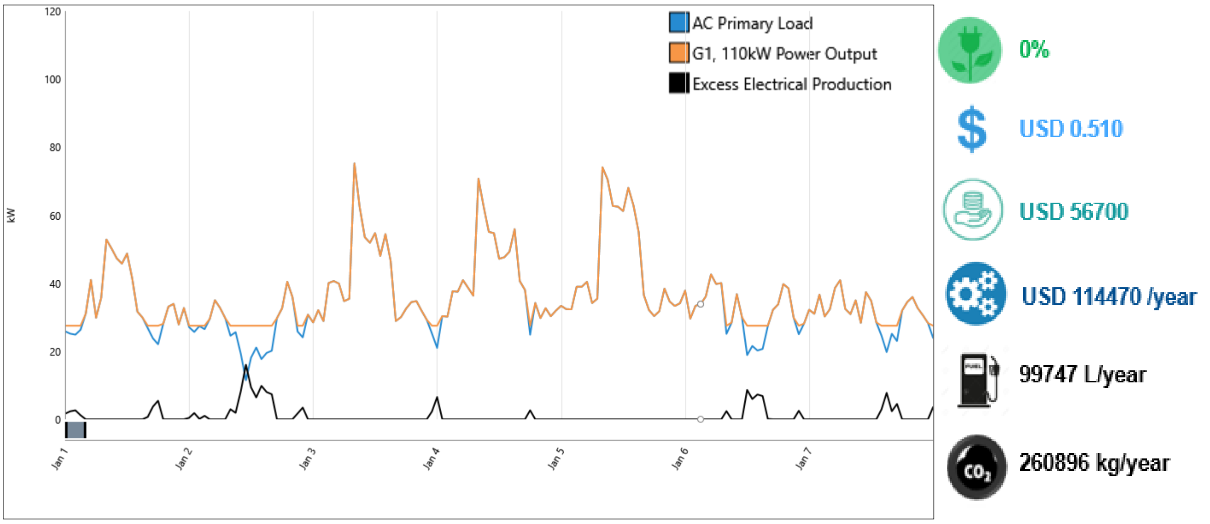

Figure 35: System Output Profile with DG

From the Figure 35, we can observe that there is excess electricity generated by DG during a certain period of the day. The reason is that the minimum load ratio for the generator was considered as 25% of the maximum capacity. Hence for 110kW, the minimum output will be 30kW (i.e., 25%*120kW). This resulted in yearly excess electricity of 20%, which in turn leads to increased fuel consumption and operating cost.

Operating a diesel generator at load levels less than 25 % of rated output for extended time periods impacts the unit negatively. The most prevalent consequence is engine exhaust slobber, which is also known as exhaust manifold slobber or wet stacking. Engine slobber is a black, oily liquid that can leak from exhaust manifold joints due to extended low or no-load scenarios. These conditions can lead to power losses, poor performance and accelerated wear of components, which can cause increased maintenance costs and unplanned downtime or failure [54].

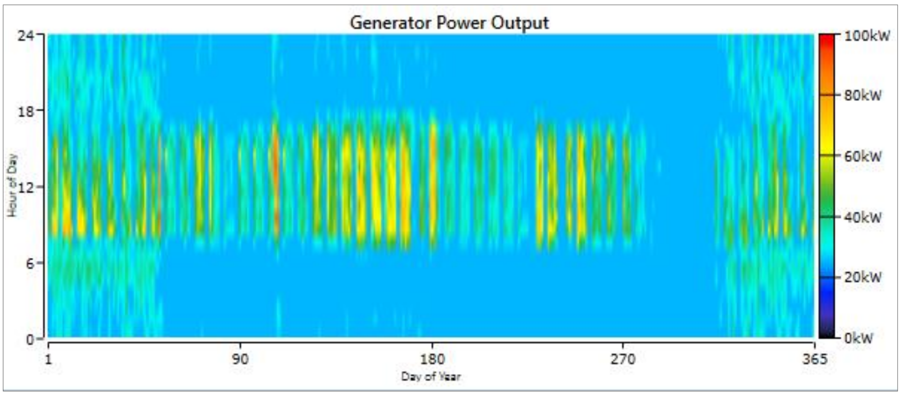

Figure 36: 110kW Generator Output

From the generator output Figure 36 above, we can observe that during most of the period in the year the generator power output is less than 60kW. Hence, considering the derating factor of 0.8 for the generator, the analysis was conducted to meet the load/peak demand by two generators of 75kW each instead of one large size generator.

6.4.2 Two Small DG

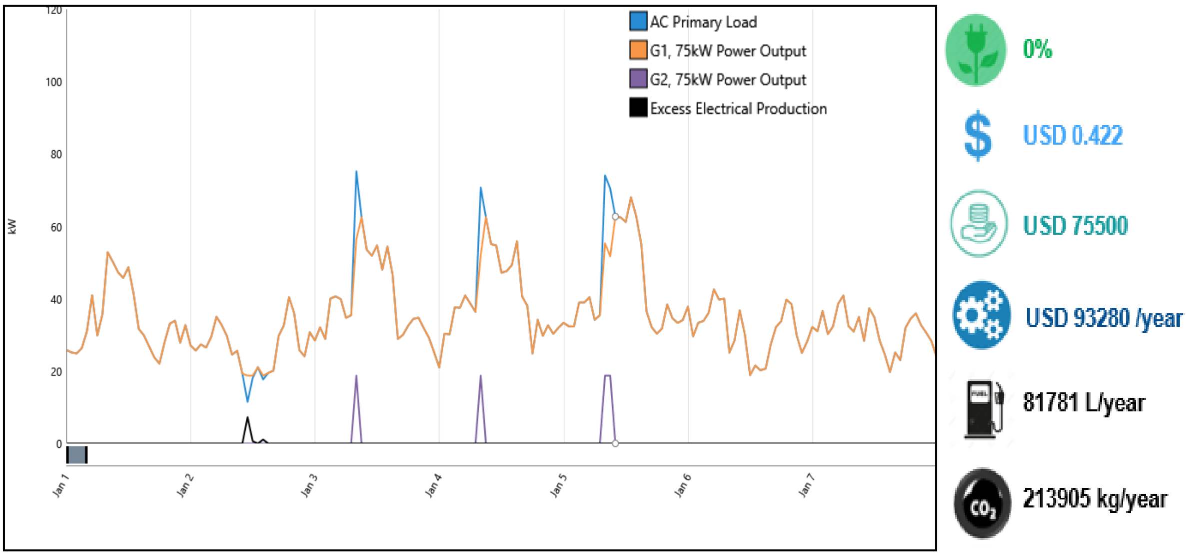

Figure 37: System Output Profile with Two DG of 75kW

Now, with each generator with a capacity of 75kW, the minimum load ratio is decreased to 19kW (25%*75kW). As we can observe in Figure 37, most of the load demand is met by one generator G1 and the second generator gets turned on only to meet peak demands. With two generators, it was possible to reduce excess electricity generation per year to less than 7% leading to decrease in fuel consumption and O&M cost. However, we can observe a slight increase in initial capital cost.

It is also to be noted that the analysis results can change based on fuel efficiency curve of generators which varies w.r.t make and capacity of the generator.

6.4.3 DG + Storage

The Kinetic Battery Model is used in Homer model to determine the amount of energy that can be absorbed or withdrawn at each time step from the storage bank. It is a two-tank model. As shown in Figure 38, the first tank contains the energy that is readily available for conversion to DC electricity. The second tank contains the energy that is chemically bound and hence not readily available for withdrawal.

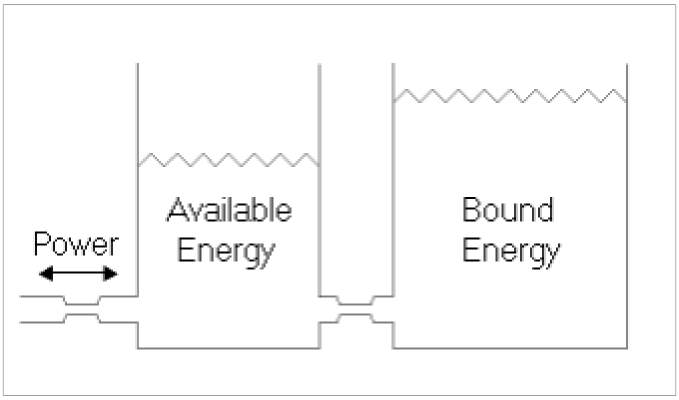

Figure 38: Two Tank Kinetic Battery Model

The maximum (or theoretical) storage capacity (Q_{max}) is the total amount of energy the two tanks can contain. The capacity ratio (*c*) is the ratio of the size of the available energy tank to the combined size of both tanks. The rate constant (*k*) relates to the conductance between the two tanks and is, therefore, a measure of how quickly the storage can convert bound energy to available energy or vice versa [55].

$$Q = Q_1 + Q_2 \tag{4}$$

Where Q1 is available energy and Q2 is the bound energy

$$Q_{1,end} = Q_1.e^{-k\Delta t} + \frac{(\mathrm{Q.k.c} - \mathrm{P})(1 - e^{-k\Delta t})}{\mathrm{k}} + \frac{\mathrm{P.c(k.\Delta t} - 1 + e^{-k\Delta t})}{\mathrm{k}} \tag{5}$$

$$Q_{2,end} = Q_2.e^{-k\Delta t} + \mathrm{Q}(1 - \mathrm{c})(1 - e^{-k\Delta t}) + \frac{\mathrm{P}(1 - \mathrm{c})(\mathrm{k.\Delta t} - 1 + e^{-k\Delta t})}{\mathrm{k}} \tag{6}$$

Where,
Q_1= the available energy [kWh] at the beginning of the time step
Q_2 = the bound energy [kWh] at the beginning of the time step
$Q_{1,end}$ = the available energy [kWh] at the end of the time step
$Q_{2,end}$ = the bound energy [kWh] at the end of the time step
P = the power [kW] into (positive) or out of (negative) the storage bank
Δt = the length of the time step [h]

The characteristics of the battery considered for simulation includes discharge rate dependent losses, temperature dependence on capacity, cycle lifetime estimation using rain-flow counting and cycle by cycle degradation based on the depth of discharge [34]. The minimum SOC for the battery is considered as 20%.

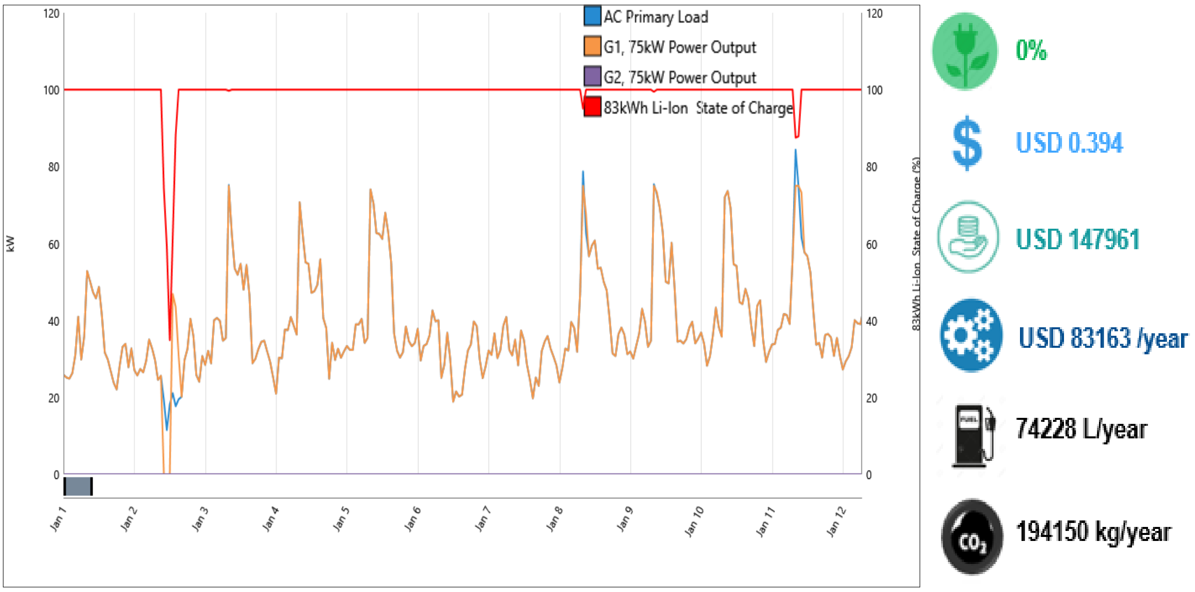

Figure 39: System Output Profile with DG+Storage

From the simulation results, as shown in Figure 39, we can observe that the output from the second generator (G1) has been now taken over by lithium-ion battery bank of capacity 83kWh. This configuration will help to achieve a further reduction in fuel consumption and overall O&M cost resulting in further reduction of LCOE.

6.4.4 DG + Storage + PV

The output from the PV array is calculated using the equation below [56]

$$P_{PV} = Y_{PV}.f_{PV}.\left[\frac{G_T}{G_{T,STC}}\right]\{1 + \alpha_P(T_c - T_{c,STC}) \qquad (7)$$

Where,

Y_{PV}= the rated capacity of the PV array
f_{PV} = the PV derating factor
G_T= the incident solar radiation on PV array in the current time step [kW/m^2]
$G_{T,STC}$= the incident solar radiation at standard test condition [1kW/m^2]
α_P = the temperature coefficient of power [%/°C]
T_c= the PV cell temperature in the current time step [°C]
$T_{c,STC}$= The PV cell temperature under standard test condition [25°C]

In section 5.4 of this report, we have analyzed the solar radiation profile, optimum tilt angle and the maximum PV (photovoltaic) capacity that can be installed at WFP office Jalalabad. Considering these input parameters along with the temperature effects, the simulation was carried out to analyze the system.

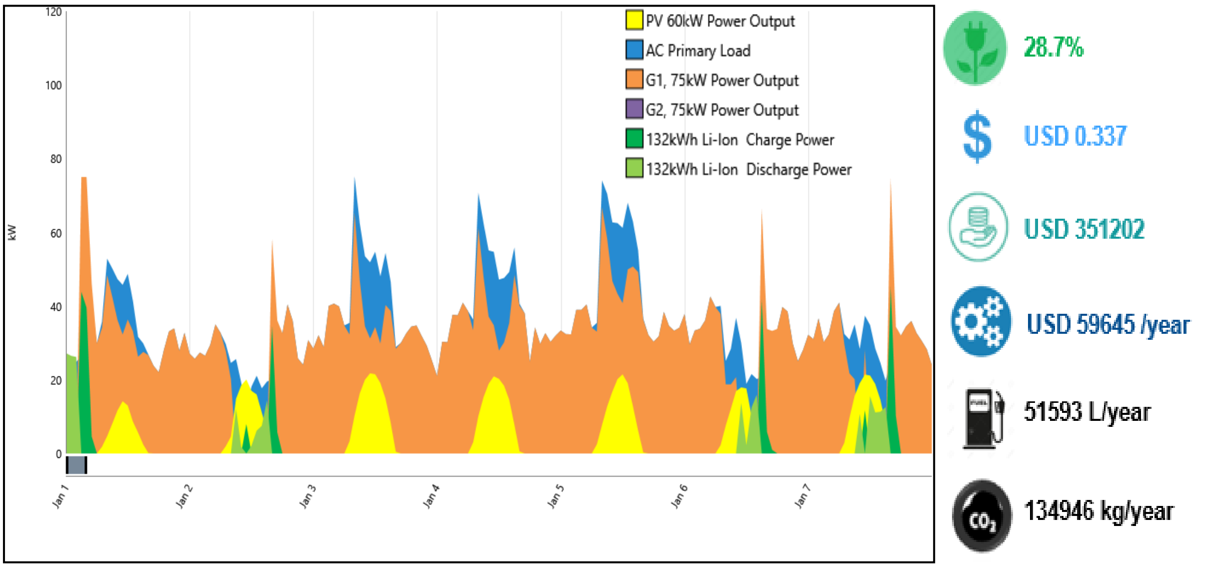

Figure 40: System Output Profile with DG+Storage+PV

With the addition of PV capacity of 60kW, we can observe that renewable penetration of 28.7% can be achieved for our system. With this configuration, we require a storage capacity of 132kWh to store and efficiently utilize the excess energy of the sun available during daytime. The capital cost has increased because of the addition of PV and storage; however, due to a significant reduction in fuel consumption, we can observe a decrease in operating cost and thus leading to the further decrease in LCOE.

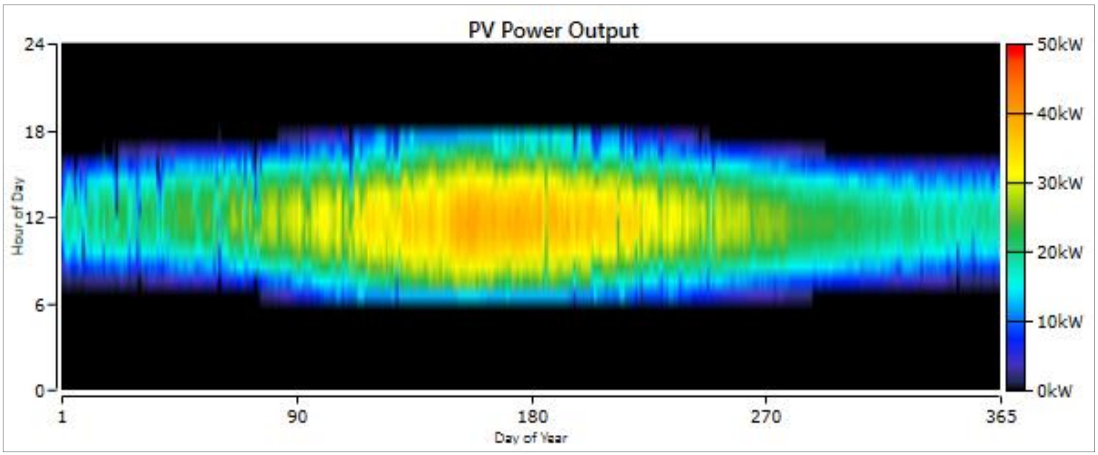

Figure 41: PV Power Output

Figure 41 shows the output from PV. As predicted, we can observe maximum output in the summer season where the solar radiation is maximum as already analyzed in Figure 22: Daily Solar Radiation (Global Horizontal).

6.4.5 DG + Storage + PV + Wind

Wind speed at a hub height of wind turbine is calculated using the equation below [57]

$$U_{hub} = U_{anem} \cdot \left[\frac{Ln(\frac{Z_{hub}}{Z_0})}{Ln(\frac{Z_{anem}}{Z_0})} \right] \tag{8}$$

Where,
U_{hub} = the wind speed at the hub height of the wind turbine [m/s]
U_{anem} = the wind speed at the anemometer height [m/s]
Z_{hub} = the hub height of the wind turbine [m]
Z_{anem} = the anemometer height [m]
Z_0 = the surface roughness length [m]
$\ln(..)$ = the natural algorithm

The wind turbine power output is given by the equation below

$$P_{WTG} = \left(\frac{\rho}{\rho_0}\right).P_{WTG,STP} \tag{9}$$

Where,
P_{WTG} = the wind turbine power output [kW]
$P_{WTG,STP}$ = the wind turbine power output at standard temperature and pressure [kW]
ρ = the actual air density [kg/m^3]
ρ_0 = the air density at standard temperature and pressure (1.225 kg/m^3)

As discussed in section 5.5, after analyzing the wind profile and Weibull distribution, it was found that the average wind speed for WFP site office Jalalabad at 50m hub height was 6m/s.

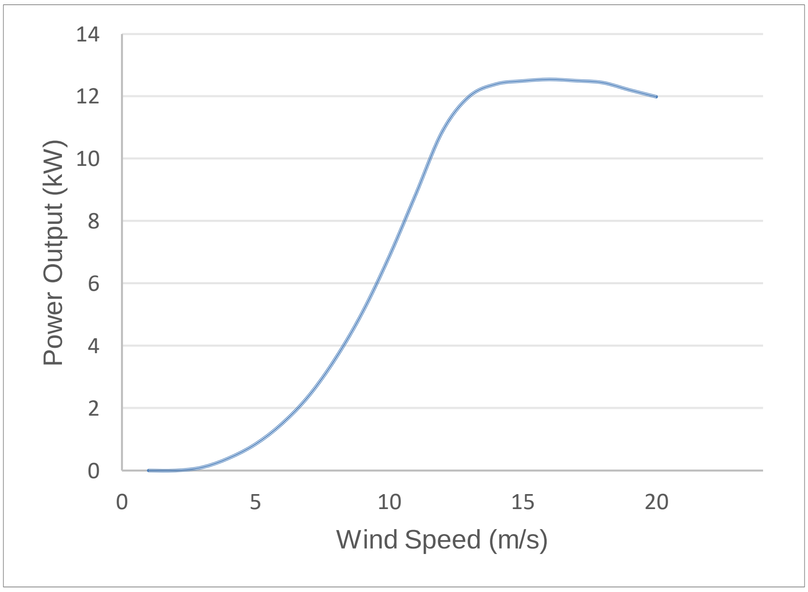

Figure 42: Power Curve of 10kW Wind Turbine

Power curves typically specify wind turbine performance under conditions of standard temperature and pressure (STP). The Figure 42 above shows the power curve plotted for Bergey Excel 10 model wind turbine. The results were obtained from wind test report with testing carried out accordance with AWEA Standard 9.1-2009. The rated power is 8.9kW at 11m/s with peak power 12.6kW at 16.5m/s. As we can observe in the figure, for an average wind speed of 6m/s we can harness only 1.51kW of energy from the wind [58]. The simulation study was carried out considering the above input wind parameters.

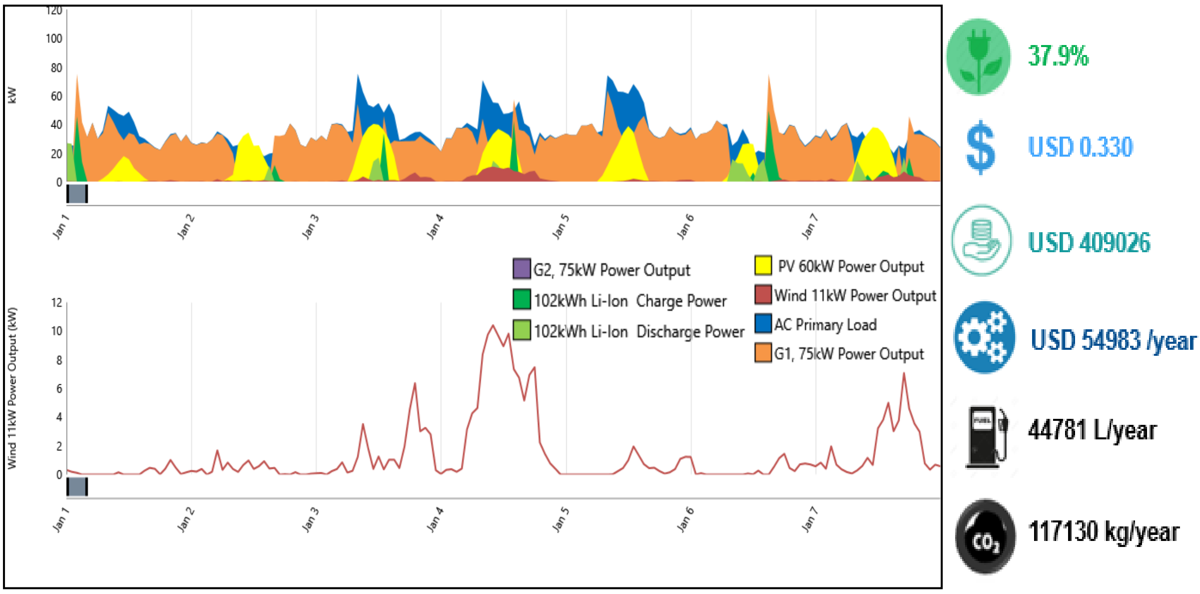

Figure 43: System Output Profile with DG+Storage+PV+WInd

From the simulation results, we can observe that with 60kW PV and 10kW wind turbine, we require lithium-ion battery capacity of 102kWh. With the inclusion of wind turbine, we were able to increase renewable penetration to 37.9%, however, there is an only slight reduction in LCOE and operating cost because of the higher O&M and capital cost of the wind turbine. We can also observe the fluctuation of wind power output in Figure 43 above.

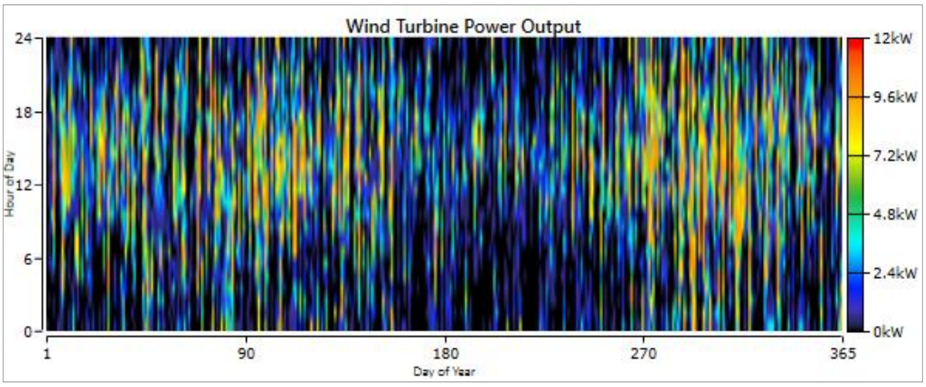

Figure 44: Wind Power Output

From Figure 44 we can observe that during most of the period throughout the year, the wind turbine output is less than 2.5kW because of low average wind speed at the site. This also resulted in not achieving significant cost savings by the inclusion of wind turbine.

6.4.6 DG + Storage + PV + Micro Hydro

The power output from the hydro turbine is given by the equation below

$$P_{hyd} = \frac{\eta_{hyd} \cdot \rho_{water} \cdot \eta_{hyd} \cdot g \cdot h_{net} \cdot \dot{Q}_{\text{turbine}}}{1000\ \text{w/Kw}} \tag{10}$$

Where,
P_{hyd} = the power output of the hydro turbine [kW]
η_{hyd} = the eefficiency of hydro turbine [%]
ρ_{water} = density of water [1000kg/m^3]
g = acceleration due to gravity [9.81m/s^2]
h_{net} = effective head [m] (can be neglected for the hydro kinetic turbine)
$\dot{Q}_{\text{turbine}}$ = hydro turbine flow rate [m^3/s]

After analyzing the percentage monthly discharge and flow velocity in section 5.6, we have come to the conclusion that the average flow velocity of the river at the site is 1.6 m/s. We have also observed that the flow velocity is maximum in the summer season and during the winter season, the velocity of river flow is too less to harness energy from microturbine.

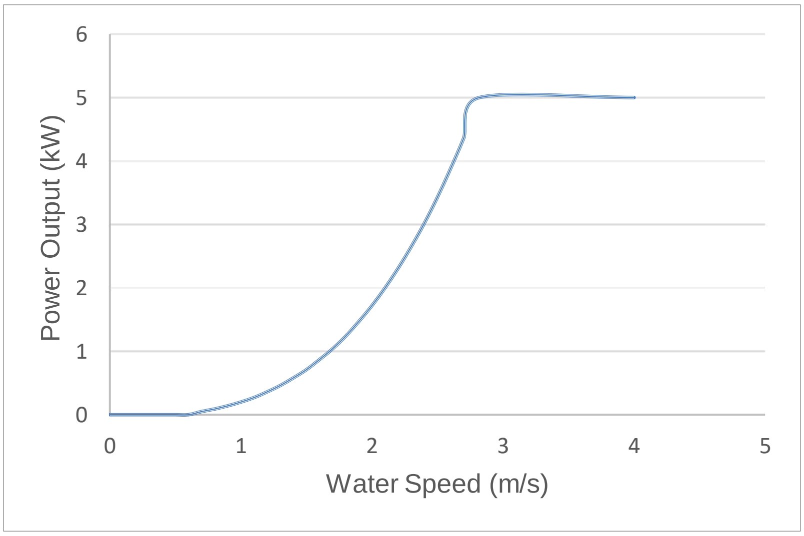

Figure 45: Power Curve of 5kW Hydrokinetic Turbine

Figure 45 shows the power curve of the 5kW micro hydro smart monofloat turbine from Smart Hydro Power Germany [19]. The maximum output from the turbine can be achieved at flow velocity 2.8m/s. The turbine parameters along with monthly flow velocity were considered in the simulation for analysis of the configuration DG + Storage + PV + Micro-hydro.

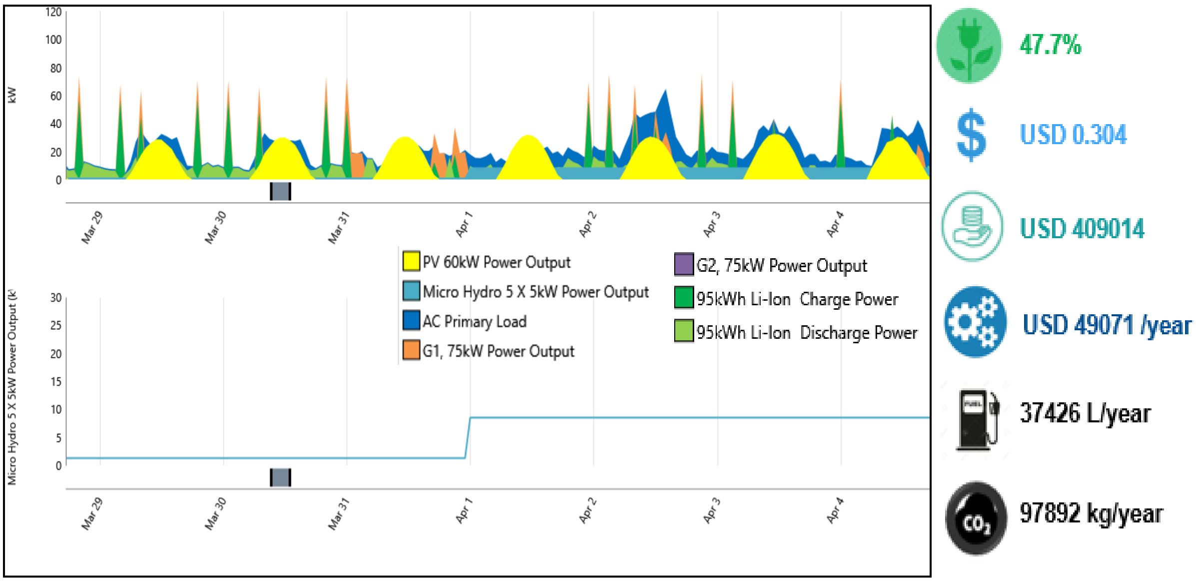

Figure 46: System Output Profile with DG+Storage+PV+MicroHydro

With the simulation study, it was found that with the installation of five hydrokinetic turbines of 5kW along with 60kW PV and 95kWh of storage we could reduce the LCOE to USD 0.304. We can also observe the decrease in operating cost and fuel consumption because of constant output power from hydro turbine throughout the day (i.e., day and night) during the summer season and thereby increasing the renewable fraction to 47.7%.

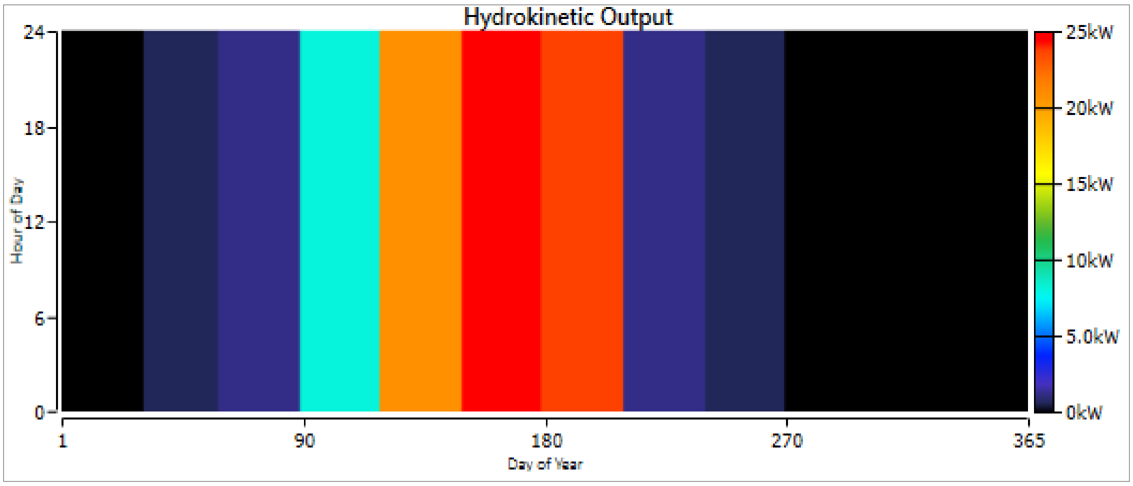

Figure 47: Hydrokinetic Yearly Output Profile

Figure 47 shows the output from hydrokinetic turbine throughout the year. Maximum output of 25kW is achieved during the month of June (summer season), whereas no output is observed during the winter season where the flow velocity is minimal. The output profile matches with flow velocity profile discussed in section 5.6.2.

6.4.7 DG + Storage + PV + Micro Hydro + Wind

A final off-grid simulation study was carried out for the whole system including all renewable energy technologies, i.e., PV, wind, and micro-hydro as shown in Figure 34.

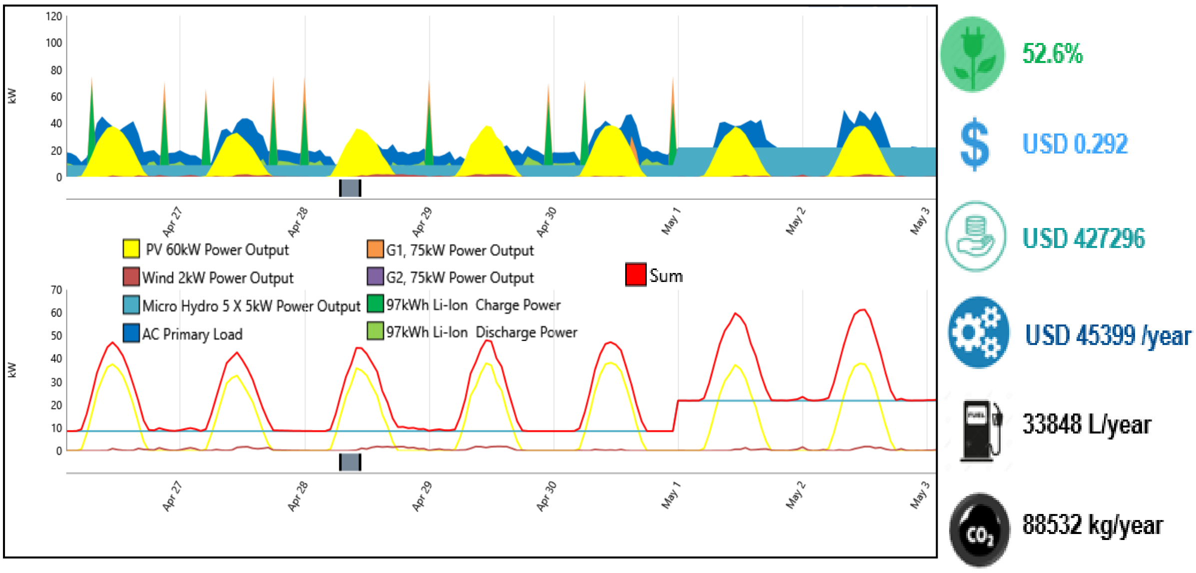

Figure 48: System Output Profile with DG+Storage+PV+Wind+MicroHydro

From Figure 48, we can observe that there is an only slight increase in a renewable fraction to 52.6% and an only slight decrease in LCOE when compared to previous case system with only micro hydro (section 6.4.6) because the contribution of the wind turbine is very minimal. The combined system requires configuration of 60kW PV, 2kW wind, 25kW micro-hydro and 97kwh of storage to run optimally.

6.4.8 Summary for Off-Grid System

Table 7 (in next page) shows the complete summary of off-grid system analysis. From the summary, we can infer that the blue highlighted last column is the cheapest option, however since the output from wind is dependent on stochastic wind profile and also the hydrokinetic turbine output depends on upstream water stream flow velocity, site survey has to be carried out to measure actual wind and water stream flow velocity to corroborate the data obtained from meteonorm and hydrological stations respectively. The depth of runoff river is also an important parameter to be considered for the installation of the hydrokinetic turbine. Due to the uncertainty of currently available data of wind and river water flow velocity, it can be said that the system highlighted with green color (i.e., **DG + Storage +PV**) is the best configuration if the WFP Jalalabad office has to be operated entirely as an off-grid system which results in yearly reduction of operating cost and CO_2 emissions up to 36%, when compared to system running with two diesel generators only.

Table 7: Summary of Off-Grid System Analysis

Icons	Large DG	Two Small DG	DG+Storage	**DG+Storage+ PV**	DG+Storage+ PV+ Wind	DG+Storage+ PV+ Micro Hydro	DG+Storage +PV+ Micro Hydro+WInd
	110 kW	2*75 kW	2*75 kW	2*75 kW	2*75 kW	2*75 kW	2*75 kW
	NA	NA	83 kWh	132 kWh	102 kWh	95 kWh	97 kWh
	NA	NA	NA	60 kW	60 kW	60 kW	60 kW
	NA	NA	NA	NA	NA	5X5 kW	5X5 kW
	NA	NA	NA	NA	11 kW	NA	2 kW
	0%	0%	0%	28.7%	37.9%	47.7%	52.6%
	$0.510	$0.422	$0.394	$0.337	$0.330	$0.304	$0.292
	$56700	$75500	$147961	$351202	$409026	$409014	$427296
	$114470 /yr.	$93280 /yr.	$83163 /yr.	$59645 /yr.	$54983/yr.	$49071 /yr.	$45399 /yr.
	99747 L/yr.	81781 L/yr.	74228 L/yr.	51593 L/yr.	44781L/yr.	37426 L/yr.	33848 L/yr.
	260896 kg/yr.	213905 kg/yr.	194150 kg/yr.	134946 kg/yrs.	117130 kg/yrs.	97892 kg/yrs.	88532 kg/yr.
	-	1.29 yrs.	5.73 yrs.	8.16 yrs.	8.41 yrs.	6.58 yrs.	6.58 yrs.

6.5 Existing Grid Connected System Analysis

In this section, we will analyze the existing system available at WFP Jalalabad office to meet the load demand and then simulate the best hybrid system configuration to achieve a reduction in operating cost and CO_2 emissions.

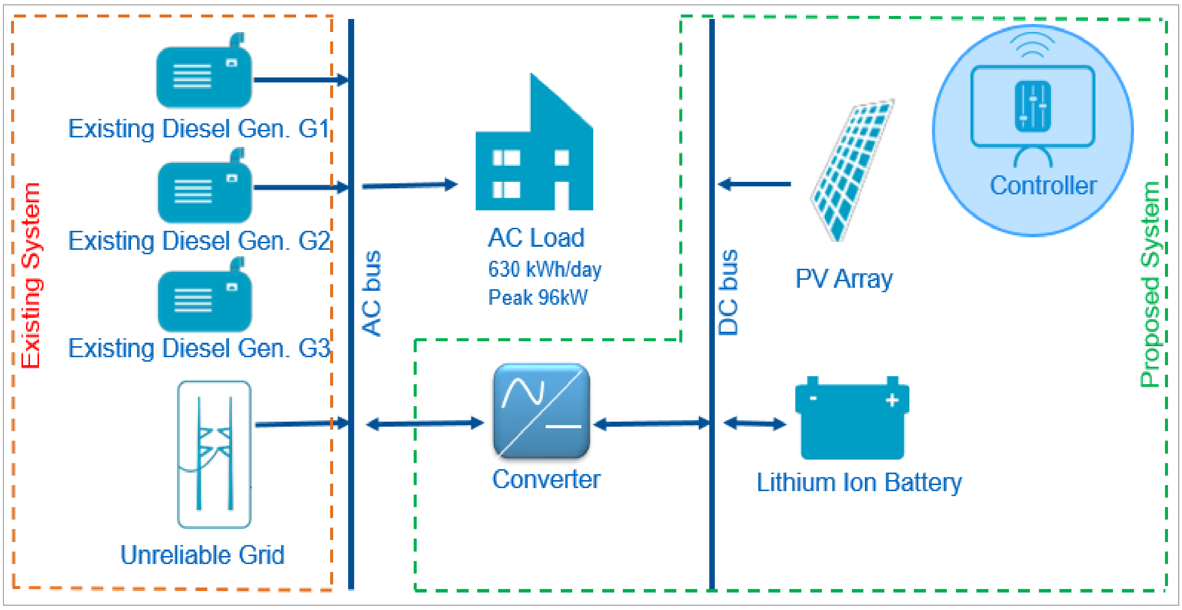

Figure 49: Grid Connected Hybrid System Layout

Currently at WFP office Jalalabad, the load demand is met by three existing generators (G1, G2, and G3) and unreliable grid as shown in Figure 49. Based on the site survey data [11] and monthly utility bills it is approximated that national grid meets around 66% of the demand and balance of which, i.e., 34% is supplied by generators.

6.5.1 Grid Parameters and Existing Generators (DG)

a) Grid Parameters

Table 8: Unreliable Grid Parameters

Parameters	
Grid Power Purchase Cost	USD 0.19/kWh
Maximum Net Grid Purchases/year	150000kWh (66% of total load demand)
Mean Outage Frequency (/year)	138
Mean Repair Time	3.8 hrs.
Repair Time Variability	30%
Grid Sales	0

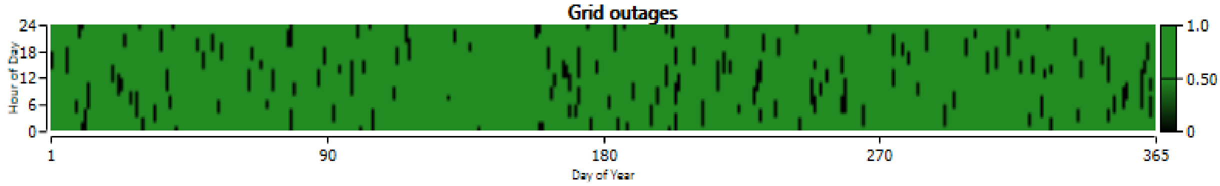

Figure 50: Figure Depicting Grid Outages throughout the Year

Table 8 indicates the grid parameters considered for the analysis. The grid reliability parameters were obtained from World Bank Group enterprise surveys database [59] as discussed with WFP team.

b) Existing Generators

As per the site survey report, the existing generators at WFP site Jalalabad are G1-150kVA, G2-165kVA, G3- 275kVA and G4-13.5kVA. The 13.5kVA is only used for server room and hence will not be considered for analysis to meet the load demand. The power factor of 0.9 was used to obtain kW rating.

6.5.2 Simulation Study of Existing DG + PV + Storage + Unreliable Grid

As indicated in Figure 49, the new system was proposed to add to the existing system. After analyzing for different configurations including the feasibility analysis of wind and micro-hydro, the optimal solution was finalized. My analysis showed that the best configuration would be **Existing DG + Unreliable Grid + 60kW PV + 35kWh of storage**.

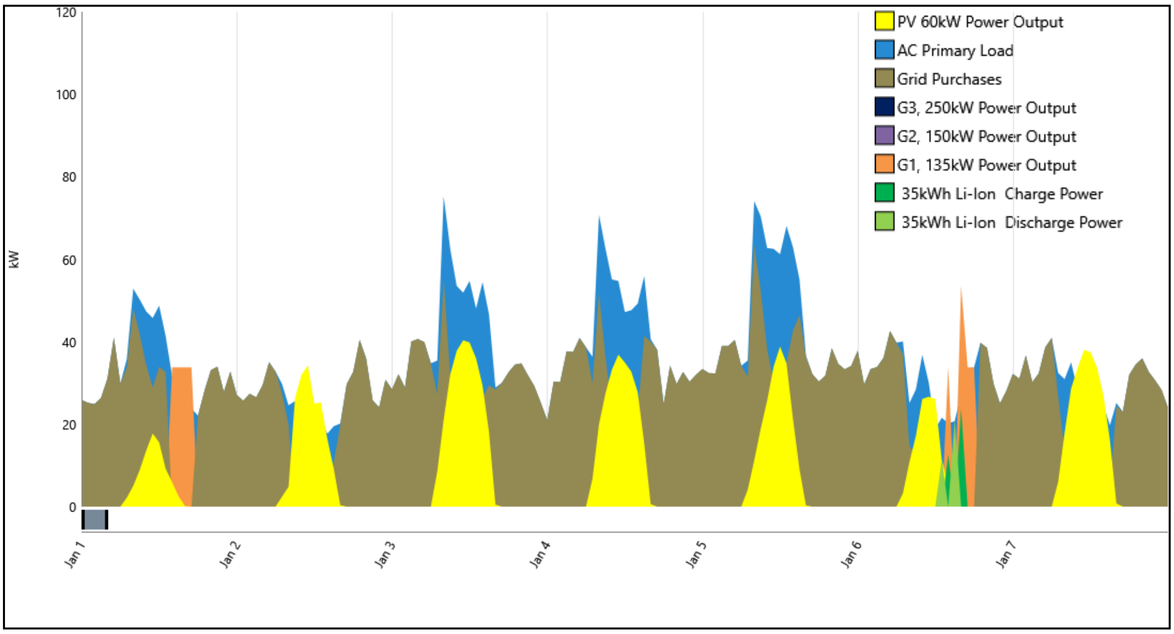

Figure 51: System Output Profile with Existing DG+Storage+PV+Unreliable Grid

As we can observe from Figure 51, most of the load demand is met by grid and PV, the batteries and generators deliver a minimal amount of load. Since the existing generators are oversized, 35kWh of storage would help to store the excess energy from generators while running at the optimum efficiency point. The cost savings with this hybrid system configuration will be analyzed under the business case in section 7.3.

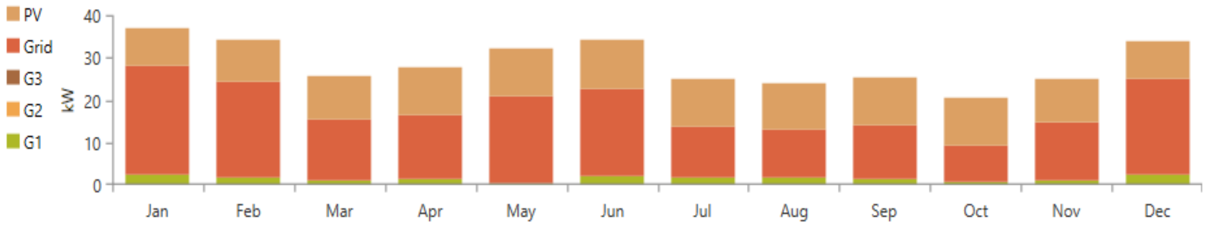

Figure 52: Monthly Average Electricity Production for On-Grid Hybrid System Jalalabad

From Figure 52 we can observe that the contribution of generators G1, G2 and G3 to meet the load demand are very minimal throughout the year. It was found through simulation that only one existing generator G1 (135kW) would operate for less than 400 hrs./year and is sufficient to meet the demand, rest of the generators have zero operational hours.

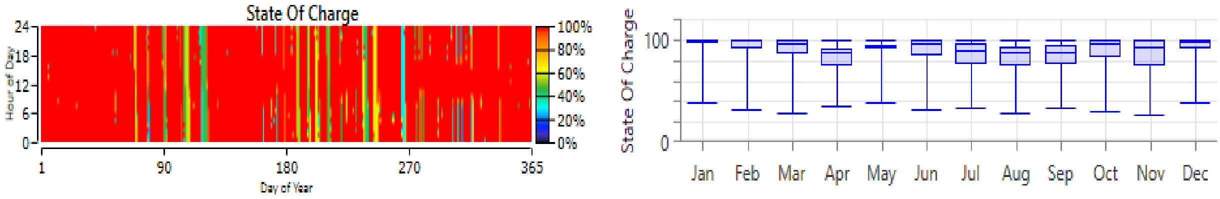

Figure 53: Daily and Monthly Fluctuation of SOC of Battery

As observed in Figure 53, the Lithium-ion battery daily SOC (for 365 days) shows >70% for most of the time during the year. The reason being, the existing generators are oversized. As a result, as soon as the generator is turned on, it runs at optimal efficiency point delivering the balance load and simultaneously charging the battery resulting in average SOC/day >70%. We can also observe monthly fluctuation of SOC varying between 20 to 100 % in the figure to the right above.

6.6 Sensitivity Analysis for Grid-Connected Hybrid System

Sensitivity analysis is used to analyze uncertainty in the output of a mathematical model corresponding to the uncertainty in its inputs, e.g., Interest rates, fuel prices, etc. [39]. All the sensitivity analysis discussed here are conducted for a hybrid system with configuration Existing DG + Unreliable Grid + 60kW PV + 35kWh of storage as discussed in section 6.5.2.

6.6.1 On Diesel Fuel Price

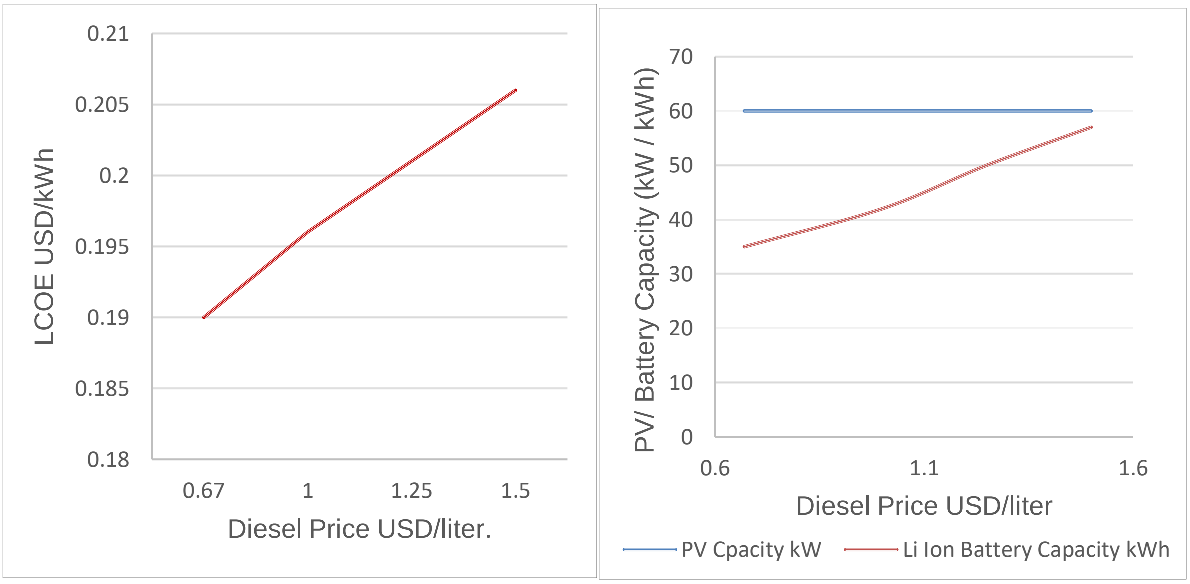

Figure 54: Graph Showing variation of LCOE, Battery Capacity Vs. Diesel Fuel Price

From Figure 54 (left), we can observe the increase in LCOE with an increase in diesel fuel prices and from figure to the right, we can observe that, for the hybrid system with the fixed PV capacity of 60kW, with the increase in diesel fuel prices, there is an increase in nominal battery capacity from 35kWh to 57kWh. The reason being, as the fuel price increases, the cost of storing energy is cheaper than running diesel generators at lower efficiency at part load.

6.6.2 On Interest/Discount Rate

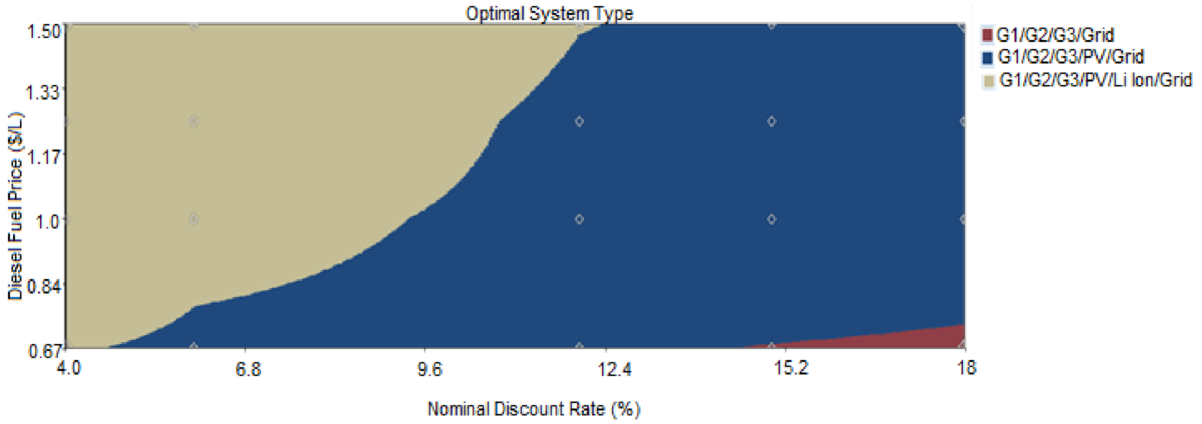

Figure 55: Sensitivity Analysis of Discount Rate

From, Figure 55 we can observe that at a lower discount rate and for all the range of fuel price the best configuration is Generators + PV+ Storage + Unreliable grid. At higher discount rates the storage can be neglected. The configuration of Existing Generators + Grid (i.e., the current existing system at Jalalabad) is only suitable for a very high discount rate above 15.2% and very low diesel price (i.e., below 0.70 USD/L).

6.6.3 On Capacity Shortage

A shortfall that occurs between the required operating capacity and the actual amount of operating capacity the system can provide is defined as capacity shortage [34].

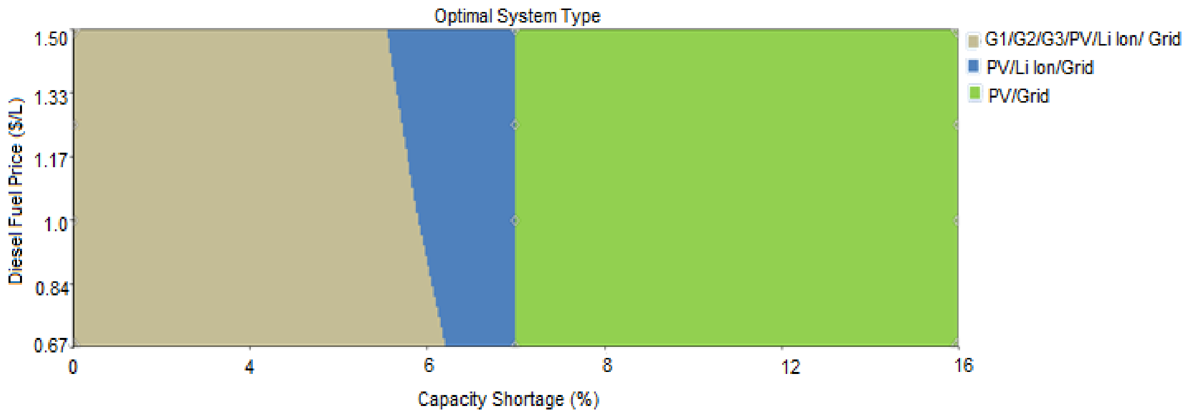

Figure 56: Sensitivity Analysis on Capacity Shortage

From Figure 56 we can infer that to have a lower capacity shortage, we have to have a hybrid system with generators and storage. However, if we allow the system to run at a higher capacity shortage, then we can rely only on PV and Grid without depending on diesel generators or storage.

6.7 Multi-Year Generator Mean Output Analysis for Load Demand Escalation:

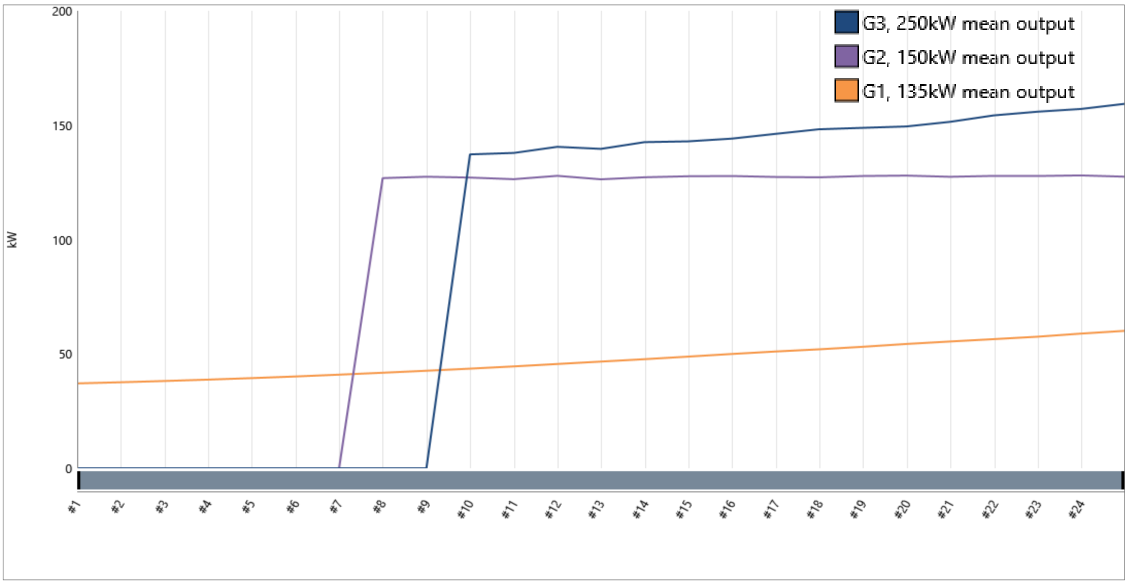

Figure 57: Existing Generators Mean Output for 4% per annum Load Escalation

An analysis was carried out to understand the existing generators mean output by taking into account 4% increase in load demand every year. As we can observe in Figure 57, the existing generators G2 and G3 will start its operation at the 7th and 9th year respectively to meet the increased load demand considering the system running with diesel generators only. It was also analyzed that if the existing generators are replaced by new ones, then three 75kW generators are required to meet the 4%/year escalated load demand.

7. Business Case

7.1 Business Canvas Model

Business model canvas is a visualizing tool for developing new or documenting existing business models. The Business Model Canvas was initially proposed by Alexander Osterwalder. Using this canvas will lead to having insights about various segments like value proposition, key activities, customer segments, revenue streams etc. [60]. Only a few segments will be discussed in this section which is relevant to my thesis.

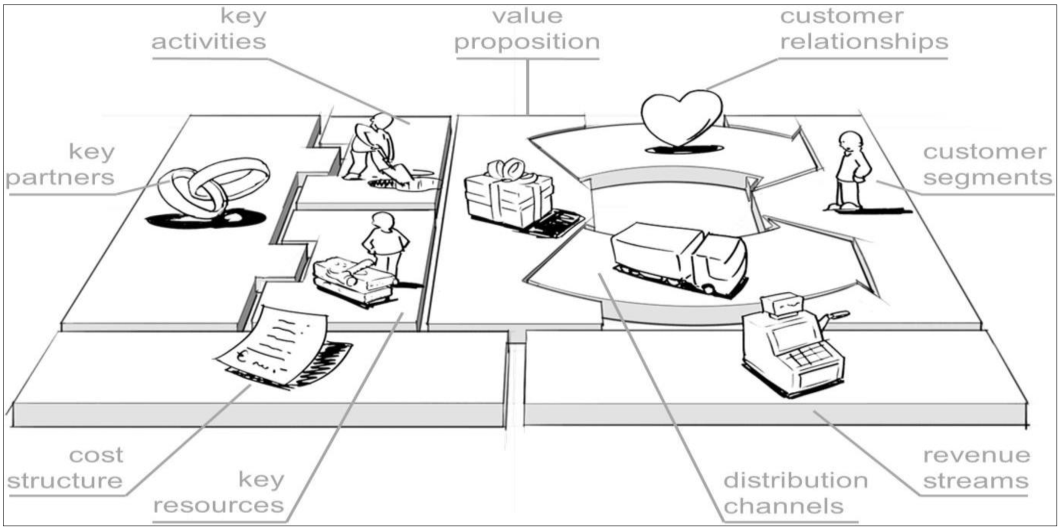

Figure 58: Business Canvas Model **[60]**

Customer segments include the customers to whom we are creating value. In case of WFP, all the WFP offices worldwide running on diesel generators having an unreliable grid or which are completely off-grid can be considered as customer segments.

The value proposition is the product, service or solution that create values to the customers. The value proposition in our business model is to reduce the operating cost of existing system run by diesel generator through the installation of the hybrid renewable system and thereby also reducing CO_2 emissions.

The key partnership includes buyer-supplier relationships or establishing collaboration with research institutes, consulting firms etc. to execute the project successfully. Market research along with frequent interactions with key suppliers was performed as a part of the thesis to identify the suitable equipment suppliers for PV, control, storage etc. WFP has already issued tenders to the shortlisted suppliers and is in the process of finalizing the key partnerships.

Key activities are the activities required to achieve our value proposition. Our key activities include site survey, feasibility study, basic and detail engineering, tendering, operation and maintenance of the system, remote monitoring etc.

7.2 Cost Parameters Definition

Various cost parameters that have been considered in my analysis are defined as below

- Levelized Cost of Energy (LCOE): It is the average cost per kWh of the useful electrical energy produced by the system.

$$\text{LCOE} = \frac{C_{ann,tot}}{E_{served}} \tag{11}$$

Where,
$C_{ann,tot}$ = total annualized cost of the system [USD/year]
E_{served} = total electrical load served [kWh/year]

- Nominal Discount/Interest Rate (i'): The rate at which one can borrow money (%).

- Real Discount Rate (i): The real discount rate is used to convert between one-time costs and annualized costs.

$$\mathrm{i} = \frac{i' - f}{\mathrm{i} + \mathrm{f}} \tag{12}$$

Where,
i = real discount rate
i' = nominal discount rate
f = expected inflation rate

- Net Present Cost (NPC): The net present cost of the component is the summation of the present value of all the cost of installing and operating the component, minus the present values of all the revenues over the project lifetime.

- Present Value (PRV): Taking into account the time value of money, the present value is the current equivalent value of a set of future cash flows.

$$\text{PRV} = \frac{\text{CF}}{(1+i)^N} \tag{13}$$

Where,
CF = future cash flows
i = the annual real discount rate [%]
N= number of years

- Annualized Cost (C_{ann}): The annualized cost of a component is the cost that, would give the same net present cost if it were to occur equally in every year of the project lifetime. It can also be termed as the cost per year of owning, operating and maintaining an asset over its entire lifetime [34] [61].

$$C_{ann} = CRF(i, R_{Proj}).C_{NPC} \tag{14}$$

Where,
C_{NPC} = the net present cost [USD]
i = the annual real discount rate [%]
R_{Proj} = the project lifetime [years]
CRF = the capital recovery factor

- Capital Recovery Factor (CRF): The ratio used to determine the present value of the annuity is known as capital recovery factor.

$$CRF(i,N) = \frac{i.(1+i^{N})}{(1+i^{N})-1} \tag{15}$$

Where,
i = real discount rate
N= number of years

- Sinking Fund Factor (SFF): The ratio used to determine the future value of a series of equal cash flow.

$$SFF(i,N) = \frac{i}{(1+i^{N})-1} \tag{16}$$

- Salvage Value (S): Salvage value is the value remaining in a component of the power system at the end of the project lifetime.

$$S = C_{rep}.\frac{R_{rem}}{R_{com}} \tag{17}$$

Where,
C_{rep} = replacement cost[USD]
R_{rem}= remaining life of component at the end of the project lifetime
R_{com} = component lifetime

- Operating Cost ($C_{operating}$): The operating cost is the annualized value of all costs and revenues other than initial capital costs.

$$C_{operating} = C_{ann,tot} - C_{ann,cap} \tag{18}$$

Where,
$C_{ann,tot}$ = the total annualized cost [USD/year]
$C_{ann,cap}$ = the total annualized capital cost [USD/year]

- Return on Investment (ROI): ROI is the rate of return on, i.e., cost saving achieved yearly on money invested. It is calculated using the equation below

$$\text{ROI} = \frac{\sum_{i=0}^{R_{proj}} \left(C_{i,ref} - C_i\right)}{\text{R}_{proj}\left(C_{cap} - C_{cap,ref}\right)} \tag{19}$$

Where,
$C_{i,ref}$, C_i= nominal cash flow for reference system and selected system
C_i = nominal cash flow for selected system i.e. best configuration
R_{proj} = project lifetime in years
C_{cap}, $C_{cap,ref}$ = capital cost of current and reference system

7.3 Business Case for Jalalabad Site

Table 9 (in next page) shows the summary of three different configurations to develop a business case. The second column indicates 1st configuration with the existing system at WFP Jalalabad office running with diesel generators only, the third column indicates 2nd configuration with existing diesel generators + 60kW PV + 35kWh storage and the fourth column indicates 3rd configuration with two new 75kW generators (i.e.by replacing the existing generators) + 60kW PV and without storage. All the systems are connected to the unreliable grid which delivers almost 60% of the total energy demand.

Table 9: Summary of On-Grid System Analysis

Icons	Existing System (1st Configuration)	**Existing DG + PV + Storage (2nd Configuration)**	New DG + PV + No Storage (3rd Configuration)
Pie Chart	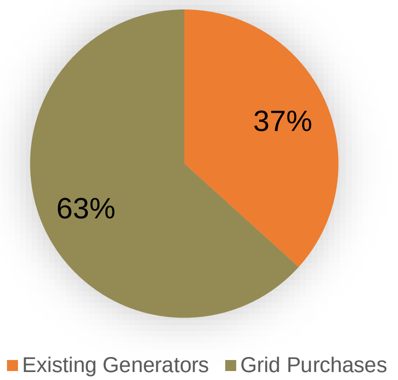	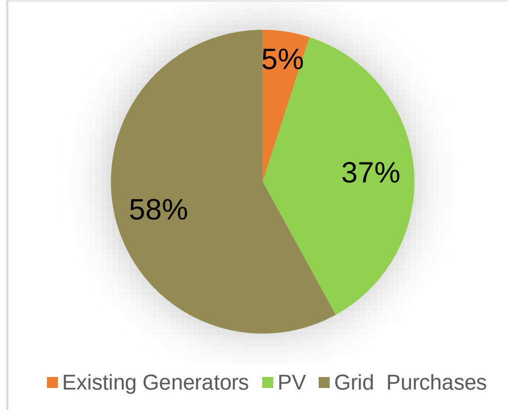	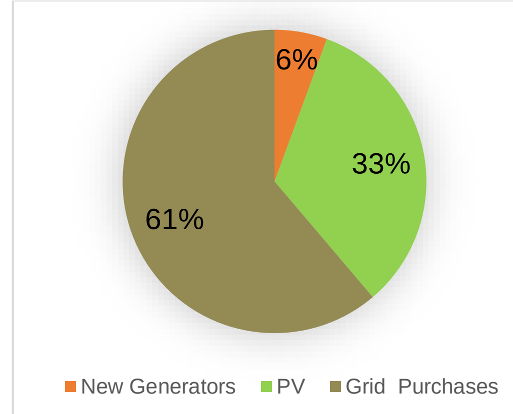
	G1=135, G2=150, G3= 250 kW	G1=135, G2=150, G3= 250 kW	G1=G2=75 kW
	NA	35 kWh	Not Required
	NA	60 kW	60 kW
	0%	31.2%	28.9%
	$0.239	$0.190	$0.201
	$5000	$200464	$243338
	$54612 /yr.	$33370 /yr.	$33722 /yr.
	29929 L/yr.	4514 L/yr.	4610 L/yr.
	78541 kg/yr.	11806 kg/yr.	12059 kg/yr.
	-	11.05 yrs.	11.26 yrs.

The 2nd configuration (highlighted with green color) is the cheapest option. The total capital cost for 2nd configuration with existing generators, PV and storage are lesser when compared to the 3rd configuration with new generators, PV without storage because no additional investment is necessary for existing generators, whereas for new generators, the initial investment is higher than investing for 35kWh storage. The advantage of investing in storage instead of new generators is that we can achieve slightly higher renewable fraction which in turn can help in reduction of diesel fuel consumption.

Comparing 2nd configuration with the existing system, from the pie chart we can observe that, with the hybrid system the share of diesel generators to meet the load has now decreased from 37% to 5% and has been replaced by PV system. ***With the 2nd configuration, we will be able to achieve approximately up to 39% reduction in operating cost and up to 85% reduction in CO_2 emissions.*** The LCOE of the proposed system is 19 cents/kWh when compared to an existing system having LCOE 24 cents/kWh. ***With the yearly cost savings achieved, WFP can help feed additional 1400 children for an entire month.***

Comparing all the configurations, we can conclude that the 2nd configuration, i.e., ***Existing Generator + PV + 35kWh storage*** is the current best solution. Since the generator runtime per year is less than 400hrs. it may not be necessary to replace the existing generators as we will not be able to achieve any significant savings. However, the health of existing generators is also an important parameter which is to be considered. If the existing generators currently running at Jalalabad WFP site have already exceeded the operational hours, then it is advisable to choose the 3rd configuration, i.e., New Generators + 60kWPV without storage.

7.3.1 Cash Flow

Cash flow is the total money flowing in and out of business. Figure 59 and Figure 60 shows the nominal cash flow by cost type and component type respectively for the best hybrid system solution (i.e., 2nd configuration) as discussed in section 7.3. From Figure 59 & Figure 60, we can observe that during the first year we require a high initial capital cost of USD 200500 for installing PV, storage, and system converter/controller. The operating cost includes the cost of grid electricity purchases, maintenance costs, and a very small fraction for diesel fuel. During the 16th year, we incur replacement cost for storage and converter which has a lifetime of 15 years. Replacement of generators was not considered due to operational time of generators being less than 400 hrs. per year. At the end of project lifetime, we can observe some salvage value contributed by components including battery and system converter which has a remaining lifetime of five years. The salvage value of generators is negligible.

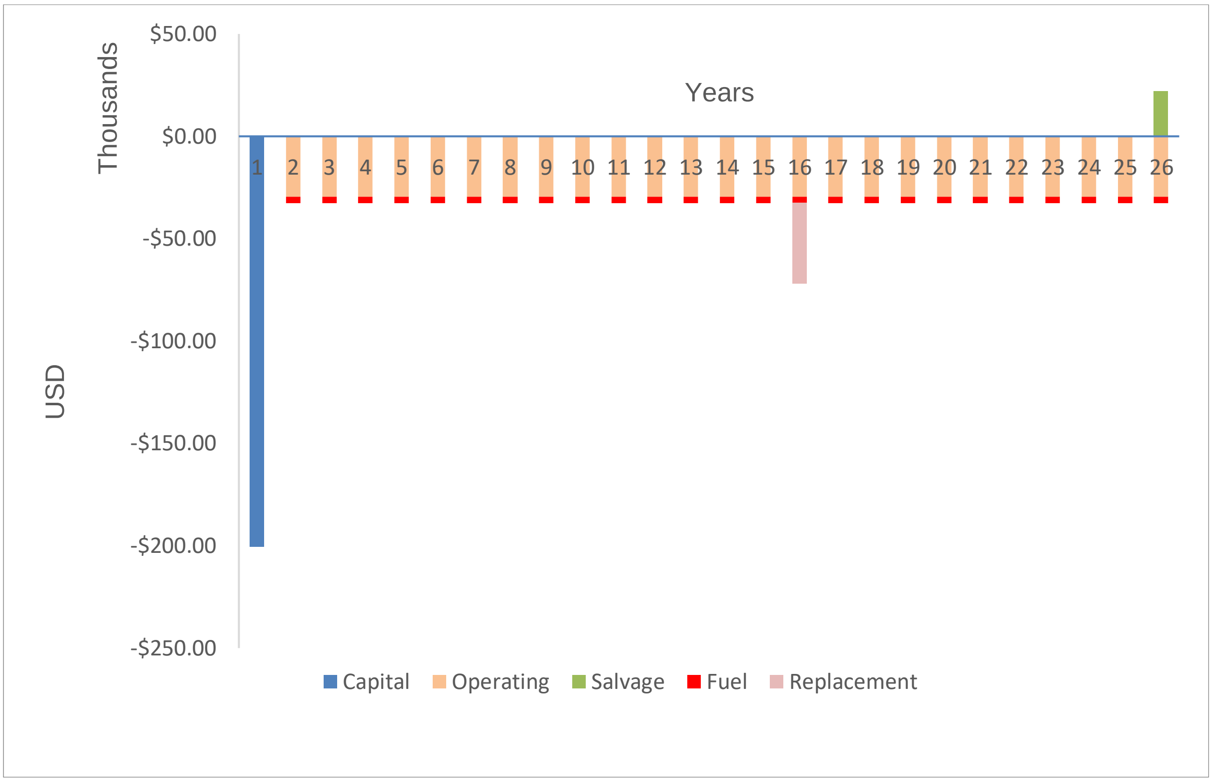

Figure 59: Nominal Cash Flow by Cost Type

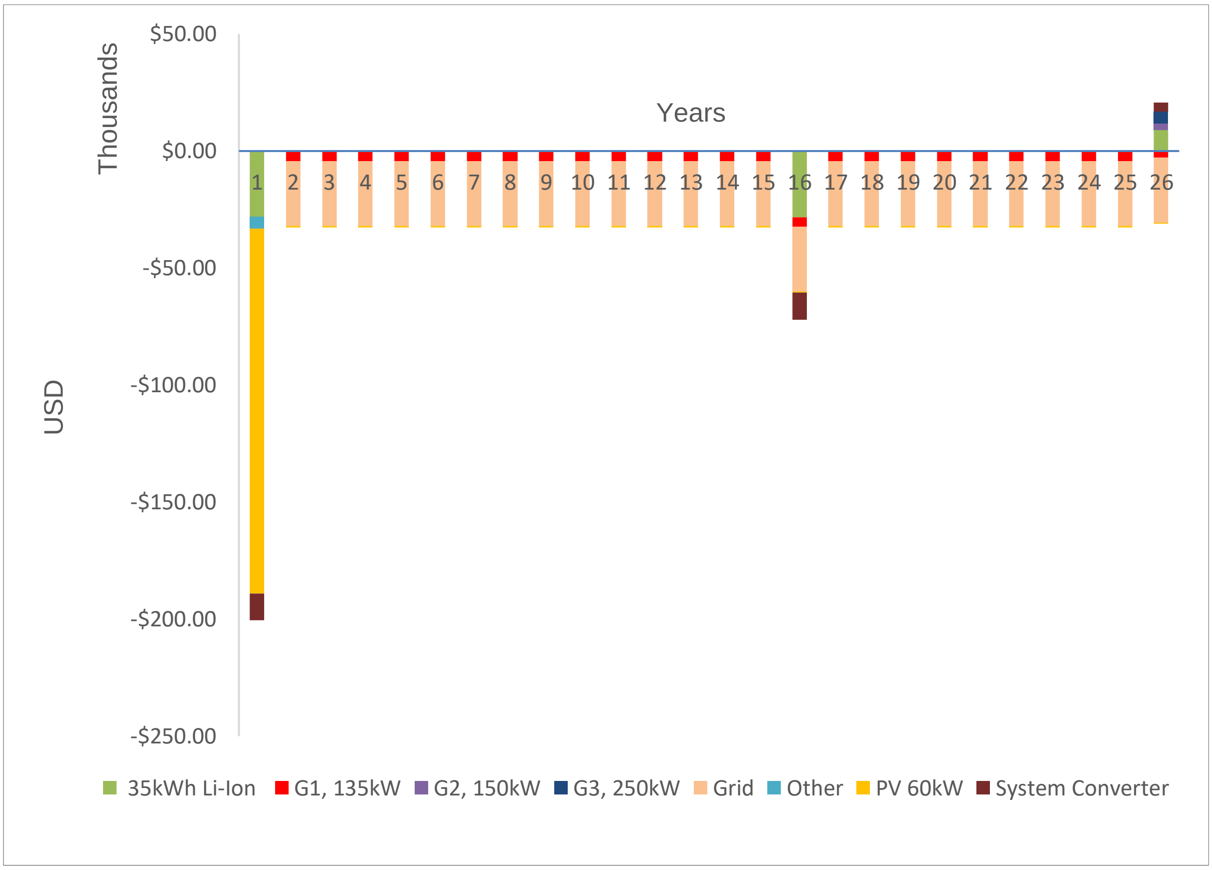

Figure 60: Nominal Cash Flow by Component Type

7.3.2 Pay Back Period

Payback period is the time duration (in years) to recover an investment. In my analysis payback period is calculated by comparing hybrid renewable system (i.e., 2nd configuration) with the existing generator only system (i.e., 1st configuration, reference system). Figure 61 shows the plot of nominal cumulative cash flow vs. years both for hybrid and existing system. We can observe that the existing system does not require high initial capital investment and therefore the nominal cumulative cash flow is less than hybrid system till it reaches **payback period of 10 years**, after which the hybrid system cash flow tends to be lower than the existing system. The discounted payback period (i.e. with discount rate) was calculated to be 11.05 years. The net present cost (NPC), return on investment (ROI) and internal rate of return (IRR) was estimated to be 0.85 Million USD, 5.6%, and 8.3% respectively. The ROI is low and the payback period is high, as no capital cost was considered for the reference system, however, in reality, there is some capital cost that was incurred while installing the generators currently running at WFP office Jalalabad.

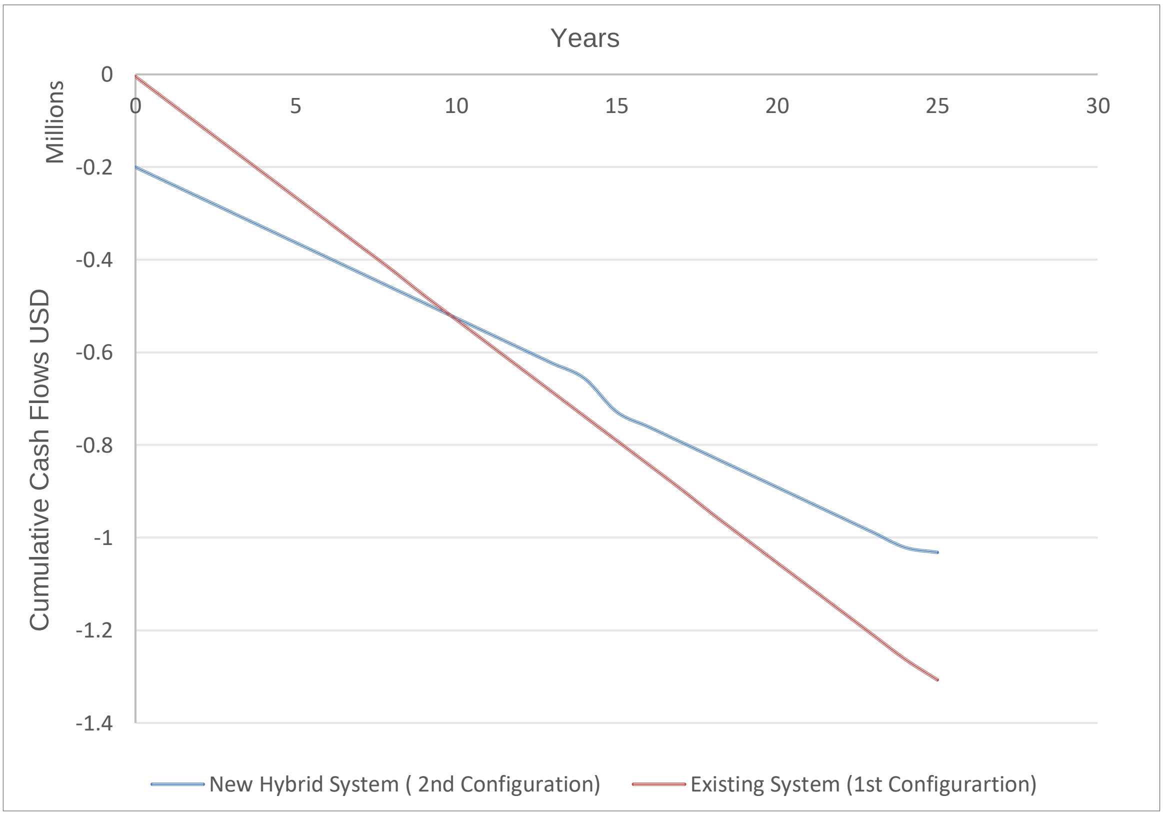

Figure 61: Nominal Cumulative Cash Flows

8. Conclusion and Outlook

The primary objective of this thesis was concept design of Type I and Type II systems to meet the energy needs of WFP remote humanitarian locations in energy efficient, reliable and environmentally friendly way. Further, market research was also carried out to identify key equipment suppliers for Type I and Type II systems considering modularity, reliability, robustness, performance guarantees, cost and maintenance parameters, etc.

Concept design of Type I systems, aimed at design and analysis of small portable systems (~32 to 40 kg) to power the biometric verification devices during the field visit by WFP team for SCOPE (WFP's central repository for beneficiary data collection and verification). Design and analysis were carried out with three different configurations depending on the size of the PV panel and battery storage capacity. As per aviation rules, it is not allowed to carry lithium-ion batteries in aircraft with a capacity exceeding 100Wh [29]. Considering battery capacity and weight constraints, the best configuration was designed with the 750Wp panel and 100Wh lithium-ion battery storage. The system was analyzed for one of the locations in sub-Saharan Africa, i.e., Chad. This system will be able to deliver 400Wh of energy during the day for 6 hrs. (from 9 to 15hrs). It is to be noted that, since the system is highly dependent on PV panel, the output from PV is subjected to the fluctuation of solar irradiance due to seasonal variation and resource location. For the system to be more reliable, it is recommended to choose the configuration with higher battery capacity, i.e., 300Wp panel with 2600Wh storage, which can deliver energy for the extended period, i.e., 8 hrs. along with the possibility of charging externally by AC source during the night. One of the small prototypes was also designed and studied to visualize the system concept. Type I systems can be customized as per WFP requirements considering battery capacity and weight constraints.

Concept design of Type II systems, aimed at design and analysis of renewable hybrid microgrid system for one of the WFP humanitarian office locations along with the business case. Feasibility analysis of various renewable technologies including battery storage was briefly studied. It was found that w.r.t biomass, the gasifier technology available for small-scale rural application, is not yet reliable and feasible for mere communal purposes and providing electricity to households and small businesses in remote [20]. Biomass power technology can generate continuous power output using many agricultural wastes, forest residues and farmers can generate income by selling biomass fuels for the local power plant. With the innovations in design and development, it can be an interesting alternative in future for small-scale electricity generation in off-grid areas of developing countries.

Off-Grid and On-Grid energy system modeling with Home Pro was carried was out for WFP Jalalabad Office, Afghanistan to meet the electricity demand by the integration of renewable energies which included analysis of load profile and integration of hourly analysis of solar, wind and micro-hydro into modeling tool along with microgrid controller, batteries, existing diesel generators, and unreliable grid parameters.

For off-grid hybrid system analysis, i.e., considering a system without having access to the grid, the analysis was carried out to determine optimal system configuration (i.e., 2*75kW DG + 97kWh of Li-Ion storage + 60kW PV+ 25kW of Micro Hydro +2kW of Wind Turbine). It was observed that because of continuous output of micro-hydro, it played a major role for an increase in the share of renewable fraction from 29%(i.e., PV + storage) to 48% (i.e., PV + storage + micro-hydro) and thereby helped in the reduction of LCOE and operating cost. However, the contribution of wind was minimal because of low wind speed and the high cost of wind turbine requiring high hub height >30m. The output from the micro-hydro and wind turbine are heavily dependent on the velocity of the water stream and wind respectively. Because of stochastic characteristics of wind and change in flow velocity based on water discharge from upstream, in situ measurement should be carried out to accurately predict the output and cost savings before implementing such technologies. PV panels can be installed only with tilt angle less than 10°to avoid inter-row shading and achieve a total capacity of 60kWp within free space available at the site. Further site survey for additional space has to be carried out if the panel has to be installed with an optimum tilt angle of 35°.

For on-grid hybrid system analysis, the unreliable grid parameters were considered along with the existing generators at WFP Jalalabad office meeting the load demand. It was analyzed that, with the existing facility more than 60% of the energy is met by unreliable grid and balance is supplied by oversized diesel generators. The analysis was performed for the possibility of installing renewables and reduce the consumption of diesel fuel. The PV capacity was restricted to 60kW because of the available free space constraints. The optimal configuration was identified as **60kW PV + 35kWh of Li-Ion Storage + Existing Generators.** With this configuration, the diesel generator run time was reduced to 5% i.e. less than 400 hrs. per year. Because of the low run time of generators, it may not be necessary to replace the existing generators with the new ones and instead invest on storage which can help to slightly increase the fraction of a renewable share, store excess energy from DG while running at best efficiency point and improve reliability. However, if the existing generators have already exceeded their lifetime, then the alternative solution is to have a system with 2*75kW DG + 60kW PV without storage.

In the **business case**, it was analyzed that the current best configuration (i.e., 60kW PV + 35kWh of Li-Ion Storage + Existing Generators) requires an initial capital investment of approximately USD 200500. With this configuration, **it is possible to achieve 39% reduction in operating cost and 85% reduction in CO_2 emissions annually.** The discounted payback period for the system is approx. 11 years calculated by comparing to the system running with existing diesel generators without capital cost. All the analysis was performed considering project lifetime of 25 years.

As per the WFP data, “USD 15 gives a 1-month supply of food to a hungry child”. With the yearly savings of 21250 USD achieved in operating cost for hybrid microgrid Type II system at Jalalabad, **WFP can help feed 1400 additional children for 1 month suffering from hunger.** With more than 300 WFP locations worldwide completely running with only diesel generators, there is enormous potential to achieve savings in operating cost and reduction in CO_2 emissions.

Outlook: It is to be noted that the optimal configuration may change in the future years depending on the innovation in technologies and advancement in research. The optimal configuration mentioned above is not a universal solution for all the WFP offices worldwide and has to be analyzed individually depending on project location, load profile, equipment usage pattern, fuel prices, project lifetime, etc. With some of the WFP emergency response services having an operational period of only a few years, the feasibility of installing such renewable hybrid system considering the payback period, return on investment, etc. has to be taken into consideration. Prediction of yearly load escalation/fluctuation should also be taken into account and is crucial to determine the optimal solution. Algorithms should be developed using machine learning and artificial intelligence to predict the load profile accurately. The possibility of installing CHP (combined heat and power) units has to be studied further to reduce the energy consumption for heating and hot water systems. It is also to be noted that the simulation output parameters, capital cost, operating cost and payback period, etc. are subjected to the change depending on input technical parameters and input cost for various technologies subjected to market price fluctuations.

List of Tables

List of Figures

List of Abbreviations and Acronyms

UN	United Nations
WFP	World Food Programme
UNDP	United Nations Development Programme
WHO	World Health Organization
EEP	Energy Efficiency Programme
SDG	Sustainable Development Goals
IEC	International Electrotechnical Commission
GIZ	Deutsche Gesellschaft für Internationale Zusammenarbeit
FAA	Federal Aviation Administration
CORDIS	Community Research and Development Information Service
NCA	Nickel Cobalt Aluminum
NMC	Nickel Manganese Cobalt
LMO	Lithium Manganese Oxide
LFP	Lithium Iron Phosphate
LTO	Lithium Titanate
PMS	Power Management System
PCS	Power Conversion System
BMS	Battery Management System
SOC	State of Charge
GCR	Ground Clearance Ratio
LCOE	Levelized Cost of Electricity
NPC	Net Present Cost
O&M	Operation and Maintenance
DG	Diesel Generator
PV	Photovoltaic
ROI	Return on Investment
IRR	Internal Rate of Return
kW	Kilowatt
kWh	Kilowatt Hours
kWp	Kilowatt Peak
AC	Alternating Current
DC	Direct Current
Hz	Hertz
CHP	Combined Heat and Power

Bibliography

[1] I. E. A. IEA, "Energy Access Outlook 2017, From Poverty to Prosperity," 2017.

[2] "International Energy Agency Database," [Online]. Available: https://www.iea.org/energyaccess/database/. [Accessed 15 April 2018].

[3] M. Allen, "WFP Energy Efficiency Program Presentation Slides," Rome, 2017.

[4] "World Food Programme," [Online]. Available: http://www1.wfp.org/. [Accessed 10 November 2017].

[5] F. D.-G. M. A.-P. F. G.-L. P. O.-R. A. S. Eduard Bullich-Massagué, "Microgrid clustering architectures," Applied Energy, vol. 212, pp. 340-361, 2018.

[6] F. I. (2015), "Current and Future Cost of Photovoltaics. Long-term Scenarios for Market Development, System Prices and LCOE of Utility-Scale PV Systems. Study on behalf of Agora Energiewende.," 2015.

[7] I. R. E. A. (IRENA), Battery Storage for Renewables: Market Status and Technology Outlook, January 2015.

[8] U. Wagner, "Thesis Description Renewable Energy System In Developing Countries for WFP Humanitarian Locations," Rome, Munich, 2017.

[9] "Innovation for Zero Hunger (WFP)," [Online]. Available: http://innovation.wfp.org/. [Accessed 20 April 2018].

[10] "WFP Energy Efficiency Survey," [Online]. Available: https://wfp.eyedro.com/. [Accessed 7 January 2018].

[11] R. Twittey, "Energy Survey Report - WFPJalalabad Office," HQ, Rome, 2017.

[12] IRENA, " IRENA Cost and Competitiveness Indicators: Rooftop Solar PV, International Renewable Energy Agency, Abu Dhabi.," 2017.

[13] T. Hamacher, TUM Lecture Notes Renewable Energy Technology II - Solar Cells, Munich: Lehrstuhl für Erneuerbare und Nachhaltige Energiesysteme, 2015.

[14] A. Gagliardi, TUM Lecture notes Nanotechnology for Energy- Solar Cells, Munich: Lehrstuhl für Nanoelektronik, 2017.

[15] "altE Store," Alternative Energy Store Inc., [Online]. Available: https://www.altestore.com/store/info/about_us/. [Accessed 1 November 2017].

[16] N. J. D. S. E. B. Tony Burton, Wind Energy Handbook, Secon Edition, John Wiley and Sons, Ltd, 2011.

[17] P. L. a. M. Koyama, "IEA ETSAP and IRENA Technology Brief E07," www.irena.org/Publications, March 2016.

[18] W. Knapp, "Lecture notes Hydro Power and Energy Storage," Chair of Hydraulic Engineering and Water Management, Munich, 2017.

[19] K. KOLMSEE, "Smart Hydro," Smart Hydro Power, [Online]. Available: http://www.smart-hydro.de/renewable-energy-solutions-developers/. [Accessed 4 November 2017].

[20] E. M. B. H. V. Dimpl, "Small-scale Electricity Generation from Biomass," GIZ HERA – Poverty-oriented Basic Energy Service, Eschborn, 2011.

[21] M. Caniato, D. Carliez and A. Thulstrup, "Challenges and opportunities of new energy schemes for food security in humanitarian contexts," Sustainable Energy Technologies and Assessments, vol. 22, no. Supplement C, p. 208–219, 2017.

[22] J. W. M. D. J. C. Xing Luo, "Overview of current development in electrical energy storage technologies and the application potential in power system operation," Applied Energy, vol. 137, pp. 511-536, 2015.

[23] "Altenenergymag," [Online]. Available: https://www.altenergymag.com. [Accessed 15 April 2018].

[24] A. Jossen, "Lecture Notes Energy Storage," Lehrstuhl für Elektrische Energiespeichertechnik, TUM, Munich, 2015.

[25] I. (2017), "Electricity Storage and Renewables: Costs and Markets to 2030, International Renewable Energy Agency, Abu Dhabi," 2017.

[26] F. Leng, C. M. Tan and M. Pecht, "Effect of Temperature on the Aging rate of Li Ion Battery Operating above Room Temperature," vol. 5, 2015.

[27] M. B. Bahman Shabani, "Theoretical Modelling Methods for Thermal Management of Batteries," vol. 8, pp. 10153-10177, 2015.

[28] "Federan Aviation Administration," [Online]. Available: https://www.ecfr.gov. [Accessed 12 April 2018].

[29] "Electronic Code of Federal Regulation," 12 April 2018. [Online]. Available: https://www.ecfr.gov.

[30] A. H. Blackwell, Encyclopedia of Science, 3rd Edition, U·X·L, 2015.

[31] "makerspace," 12 April 2018. [Online]. Available: https://www.maker-space.de/.

[32] "European Commission," [Online]. Available: https://cordis.europa.eu/project/rcn/67577_en.html. [Accessed 14 April 2018].

[33] J. K. P. B. Amandeep Kaur, "A review on microgrid central controller," Renewable and Sustainable Energy Reviews, vol. 55, pp. 338-345, 2016.

[34] "Homer Energy," [Online]. Available: https://www.homerenergy.com. [Accessed 10 January 2018].

[35] P. Bauer, "Lecture Notes on Microgrid Layouts," Delft University of Technology, Delft, 2018.

[36] M. Alen, "WFP Liberia EEP Project System Technical Design," Rome, 2018.

[37] E. F. G. G. R. G.-M. Iván Patrao, "Microgrid architectures for low voltage distributed generation," Renewable and Sustainable Energy Reviews, vol. 43, pp. 415-424, 2015.

[38] "Institutional Development for Energy in Afghanistan (IDEA) Programme, Enabling PV Afghanistan," Deutsche Gesellschaft für Internationale Zusammenarbeit (GIZ), 2017.

[39] "Wikipedia," [Online]. Available: https://www.wikipedia.org/. [Accessed 14 April 2018].

[40] "Meteonorm," [Online]. Available: http://www.meteonorm.com/. [Accessed 5 January 2017].

[41] K. N. Y. H. J. S. H. W. D. Y. Ruidong Xu, "Analysis of the optimum tilt angle for a soiled PV panel," Energy Conversion and Management, vol. 148, pp. 100-109, 2017.

[42] M. A. R. Y. A. A.-T. Tarek O. Kaddoura, "On the estimation of the optimum tilt angle of PV panel in Saudi Arabia," Renewable and Sustainable Energy Reviews, vol. 65, pp. 626-634, 2016.

[43] "PVsyst," [Online]. Available: http://www.pvsyst.com/en/. [Accessed 10 January 2018].

[44] J. B. Matthew Culligan, "Impact of Tilt Angle on System Economics," SUNPOWER, San Jose, CA, 2007.

[45] "CIVICSOLAR," [Online]. Available: https://www.civicsolar.com. [Accessed 10 April 2018].

[46] "HelioScope," [Online]. Available: https://www.helioscope.com. [Accessed 13 April 2018].

[47] R. S. Anuj Kumar, "Performance analysis of a Savonius hydrokinetic turbine having twisted blades," Renewable Energy, vol. 108, pp. 502-522, 2017.

[48] A. M. Marketa Hulpachova, "Water management of the Kabul River Basin in Afghanistan and Pakistan," Media in Cooperation and Transition (MiCT), Germany, 2015.

[49] K. KONISHI, "Draft Kabul City Master Plan," RECS International Inc. Yachiyo Engineering Co., Ltd., 2011.

[50] S. F. Trevor Porter, "Pollution and the Kabul River, An Analysis and Action Plan," Department of Environmental Planning and Management Peshawar University.

[51] Y. E. C. L. C. E. I. C. L. S. C. I. RECS International Inc, "The Study for the development of the master plan for the Kabul Metropolitan area in the Islamic Republic of Afghanistan," Japan International Cooperation Agency (JICA), 2009.

[52] G. H. Torge Tunnermeier, "Hydrogeology of the Kabul Basin," 2005.

[53] "Renewable Power Generation Costs in 2017," International Renewable Energy Agency (IRENA), 2018.

[54] B. Jabeck, "The Impact of Generator Set Underloading," Caterpillar, 2014.

[55] M. J. Manwell JF, "Lead acid storage model for hybrid energy systems," Solar Energy, vol. 50, pp. 399-405, 1993.

[56] B. W. Duffie JA, Solar Engineering of Thermal Processes 2nd edition, Wiley, New York, NY, 1991.

[57] M. J. R. A. Manwell JF, Wind Energy Explained, Wiley, New York, NY, 2002.

[58] "Small WInd Certification Council," [Online]. Available: smallwindcertification.org. [Accessed 10 January 2018].

[59] "World Bank Group Enterprise Survey Database," [Online]. Available: http://www.enterprisesurveys.org. [Accessed 15 January 2018].

[60] A. Osterwalder, Y. Pigneur and T. Clark, Business model generation, Hoboken, N.J.: John Wiley & Sons, 2010.

[61] "Investopedia," [Online]. Available: https://www.investopedia.com. [Accessed 15 April 2018].